
Detrimental effects of UV-A radiation on antioxidant capacity and photosynthetic efficiency on a tropical microalga

Isaia Anna ^{1,2}, Coulombier Noémie ³, Le Dean Loic ¹, Meriot Vincent ⁴, Jauffrais Thierry ^{1,*}

¹ Ifremer, IRD, Univ Nouvelle-Calédonie, Univ La Réunion, CNRS, UMR 9220 ENTROPIE, RBE/LEAD, 101 Promenade Roger Laroque, Noumea 98897, New Caledonia

² Univ Brest, CNRS, IRD, Ifremer, LEMAR, Plouzané F-29280, France

³ ADECAL Technopole, 1 bis rue Berthelot, Noumea 98846, New Caledonia

⁴ ISEA, EA7484, Université de Nouvelle Calédonie, Campus de Nouville, Nouméa 98851, New Caledonia

* Corresponding author : Thierry Jauffrais, email address : Thierry.Jauffrais@ifremer.fr

anna.isaia@univ-brest.fr ; noemie.coulombier@adecal.nc ; loic.le.dean@ifremer.fr ; vincent.meriot@etudiant.unc.nc

Abstract :

Antioxidants are molecules able to neutralize reactive oxygen species with potential applications in the cosmetic or nutraceutical industries. Abiotic stressors, such as light intensity, ultraviolet (UV) radiation, or nutrient availability, can influence their production. In the perspective of optimizing and understanding the antioxidant capacity of microalgae, we investigated the effects of UV-A radiation on growth, and antioxidant and photosynthetic activities on *Tetraselmis*, a microalga genus known for its high antioxidant capacity. Cultures were exposed to UV-A radiation alongside to photosynthetically active radiation (PAR) in photobioreactors operated in continuous culture. UV-A exposure affects both the photosynthetic and antioxidant activities of *Tetraselmis*. Photosynthetic parameters suggest that UV-A has a negative effect on photosynthetic efficiency, particularly on the electron transport chain on short-term exposure (1–2 days). However, a resilience of most physiological parameters was observed over the experiment (10 days) suggesting a photochemical adaption over long-term exposure to UV-A radiation. Concerning the antioxidant capacity, UV-A exposure reduced the antioxidant capacity in *Tetraselmis* suggesting the use of antioxidant molecules to counteract reactive oxygen species production and prevent damage to photosystem II. Finally, the highest antioxidant capacity never observed with a *Tetraselmis* sp. was measured in cultures without UV addition, with an IC₅₀ of $2.87 \pm 0.24 \mu\text{g mL}^{-1}$, a value close to the reference compounds Trolox and α -tocopherol. This study showed the great potential of *Tetraselmis* as a source of antioxidants under favorable culture condition and without UV-A radiations. Indeed, we discourage the use of UV-A to enhance antioxidant capacity in this species due to its negative impact on it and on the photosynthetic efficiency.

Highlights

► High antioxidant activity of *Tetraselmis* under favourable culture condition. ► The photosynthetic apparatus of *Tetraselmis* is resilient to UV-A exposure. ► UV-A exposure reduce antioxidant activity of *Tetraselmis*.

Keywords : Microalgae, Photophysiology, Photosynthesis, TBARS assay, Antioxidant activity, Phytoplankton, Chlorophyll a fluorescence, Pulse amplitude modulated fluorometry, PAM

1. Introduction

In recent years, interest in molecules of natural origin has increased [1,2]. In this perspective, microalgae are getting increasing attention as a potential source to meet this growing demand [3,4]. They are a diverse group of photosynthetic microscopic organism and function as real cellular factories able to produce an array of valuable compounds including fatty acids, pigments, and vitamins [5–7]. These molecules can have bioactive properties such as antibacterial, antifungal and/or antioxidant activities [8–13] with potential applications in human and animal nutrition, pharmaceuticals, or cosmetics [11,14–16].

Among these molecules of interest, there is a growing demand for natural antioxidant molecules in the cosmetic, pharmaceutical and/or nutraceutical industries [6]. These compounds play a major role in regulating the production of reactive oxygen species (ROS) and their synthesis can be oriented by various abiotic stressors [17,18]. Indeed, stressors such as light, pH, nutrient availability, temperature, and UV exposure have been suggested to influence antioxidant production and capacity [19–22]. Solar light, although essential for microalgae, can be identified as a stress factor. It is composed of a wide range of radiations from infrared to UV radiations through visible light. UV radiations are known to be harmful causing damage to cell components of most living organisms through direct absorption targeting in majority DNA and protein complexes such as photosystem II (PSII) reaction centers (RCs). In addition, UV radiations, especially UV-A, can indirectly damage the cell through the production of ROS [23,24]. To counteract such formation, studies have suggested that microalgae exhibit an antioxidant response through the induction and accumulation of carotenoids [25–28] and fatty acids [25]. Despite UV-A being the most penetrating radiation in the atmosphere and the water column [24,29,30], further studies targeting the physiological responses of microalgae to UV-A are still needed. To monitor the impact of UV-A on microalgae physiology, specifically on their photochemistry (mainly PSII), pulse amplitude modulated (PAM) fluorometry was used. This widely used technique based on chlorophyll fluorescence, offers the advantage to be fast and non-invasive to follow culture fitness [31,32]. PAM fluorometry measures the light energy emitted by the light-harvesting pigments

associated with photosynthesis. In short, the light energy absorbed by chlorophyll is either used for photosynthesis, dissipated as heat (excess energy), or re-emitted (fluorescence). Therefore, by measuring the fluorescence yield, information about the PSII photosynthetic efficiency can be retrieved [33,34].

In this context, we examined the relationship between antioxidant and photosynthetic activities to evaluate the effect of UV-A radiation on microalgae physiology. We addressed this issue using a *Tetraselmis* sp. isolated in New Caledonia [35]. This genus is found in a wide range of habitats, from freshwater to marine ecosystems [36]. It is getting attention due to its ability, among other things, to produce bioactive molecules, making it a valuable microalga in animal feed, cosmetics, pharmaceuticals, and nutraceuticals [14–16,37]. Some of these molecules such as phenolic compounds [38], pigments [19] and vitamins [39] have antioxidant properties. Therefore, with the overall objective of optimizing antioxidant capacity and biomass production, the present study aims to assess the impact of UV-A exposure on *Tetraselmis* sp. growth, photosynthetic and antioxidant activities.

2. Material & Methods

2.1. *Microalga culture*

Tetraselmis sp. (N3C05) was isolated from coastal seawater in New Caledonia, a French archipelago in the Pacific Ocean, characterized by a tropical weather [35,40,41]. The inoculum was grown in a 1 000 mL Erlenmeyer flask with a working volume of 400 mL, in Conway-enriched seawater (See composition in Table A1, appendices data, [42]), under continuous aeration, illumination ($50 \mu\text{mol photons m}^{-2} \text{s}^{-1}$) and with daily homogenization.

2.2. *Experimental culture conditions*

The cultures were produced in two 2.5 L photobioreactors (PBR) made of transparent polymethylmethacrylate (PMMA). After 20 minutes of sterilization using 0.5% DEPTIL PA5 (biocid agent with 5% peracetic acid, Kersia group, France) and two rinses with filtered seawater ($0.2 \mu\text{m}$), the PBRs

were inoculated with 200 mL of *Tetraselmis* in filtered seawater (0.2 μm) enriched with 1 mL L⁻¹ of Conway medium [42]. After inoculation, the initial cell concentration in the PBRs was $2.37 \pm 3.01 \cdot 10^5$ cells mL⁻¹. For the first 36 hours, the cultures were maintained in batch culture condition. Subsequently, the cultures were operated in continuous culture condition with a constant inflow of fresh medium (*i.e.* filtered seawater (0.2 μm) enriched with Conway medium (1 mL L⁻¹) with additional NaNO₃ (4 mL L⁻¹ of a stock solution at 100 g L⁻¹) to prevent nitrogen limitation) and a constant outflow of culture. The cultures were operated at a 0.7 day⁻¹ dilution rate and were exposed to UV-A for 10 days. Throughout the experiment, the cultures were maintained in continuous culture, at pH 8.0 with CO₂ injection, and at a temperature of 26 °C. An Arduino electronic card was used to set these conditions and they were monitored thanks to a Raspberry PI computer. One side of the PBR was exposed constantly to 50 $\mu\text{mol photons m}^{-2} \text{ s}^{-1}$ using fluorescent tubes (OSRAM cool 109 daylight HO24W/965). Culture homogenization was achieved with a Rushton turbine at 90 rpm and aeration was performed by bubbling the culture with 0.2 μm filtered air.

When the culture in PBRs reach steady state (*i.e.* cell concentration and absorbance remained constant for at least three consecutive days) the UV-A treatment was applied over a period of 10 days. To allow the UV-A exposure, the culture went through a UV system using glass tubes, forming a loop connected to the PBRs (See scheme of the PBR set up in Fig. A1, appendices data). The UV radiation source consisted in a total of 8 LEDs (LED UV, UV5TZ-385-15) per loop, emitting light at a peak wavelength of 385 nm (min 382.5, max 387.5, viewing angle 15°). A constant illumination was kept throughout the experiment at an intensity of 1 480 W m⁻², as measured with a UV captor from Adafruit industries (RS-124-5472). The flow rate inside the UV system was set at 6.25 mL min⁻¹. During this experiment, all measurements were done before UV-A exposure (day 0, initial state = control condition) and during the UV-A exposure (from day 1 to day 10 depending on the parameter).

2.3. Cell growth measurements

To monitor cell growth, daily measurements of light absorbance were conducted using spectrophotometry at 680 nm (UV mini-1240 spectrophotometer, Shimadzu, Japan), which measures

pigment absorption (chlorophyll *a*, Chl *a*). In addition, cell concentration was estimated daily using a Malassez hemocytometer (Paul Marienfeld GmbH & Co. KG, Germany) under an optical microscope.

2.4. *Elemental analysis*

The nitrogen and carbon status of *Tetraselmis* were assessed using 3-4 mL aliquots of the culture medium collected before (day 0) and during the UV treatment (after 2 and 10 days), which were filtered through glass fiber filters (1.2 μm , Whatman GF/C 25 mm). Then, the filters were dried at 70°C for at least 24 hours in glass Petri dishes and stored at -20°C until analysis. To prevent carbon or nitrogen contamination, all equipment was pre-combusted in a furnace at 450°C for 4 hours before use. Sample analyses were performed using an elemental analyzer (SERCON Integra 2, United Kingdom). The C:N ratio was calculated by dividing the cell carbon content (QC) by the cell nitrogen content (QN).

2.5. *Photosynthetic parameters*

To assess the photophysiological state of the cultures, the maximum quantum efficiency of PSII (F_v/F_m), fluorescence transient (OJIP, [43]), rapid light curves (RLC, [44]) and Non-Photochemical Quenching (NPQ) were measured using a Pulse Amplitude Modulated (PAM) fluorometer (AquaPen-P AP 110-P of Photon Systems Instruments, Czech Republic). It is a non-destructive technique based on the Chl *a* fluorescence, with a blue excitation light at 455 nm, which allows the monitoring of the culture's photosynthetic activity. PAM fluorometry is a powerful and widely used technique [45–48]. This method offers the advantages of being rapid and non-invasive [46]. In this context, Rapid Light Curves (RLCs) have been employed to optimize growth and assess the impact of environmental factors on photosynthetic electron flow regulation in microalgae [48–50], including for *Tetraselmis* [20]. However, it is important to note that although PAM fluorometry has proven to be a valuable tool for studying microalgal photophysiology, it is often considered biased due to: (1) variations in fluorescence signals by the sample, often caused by the thickness of macroalgal tissues, which can hinder direct comparison with oxygenic photosynthesis measurements, especially at high irradiance; and (2) the time required to reach photosynthetic steady-state, which may limit its applicability under certain

conditions (reviewed in Enriquez and Borovitzka,[51]). Despite these limitations, the use of relative electron transport rate (rETR) values instead of absolute ETR is recommended to mitigate issues associated with absorbance (*i.e.*, the fraction of incident light absorbed by pigmented tissue), particularly when the organisms or tissues under examination have similar absorption cross-sections [51–53]. Moreover, in our study, Ft remained relatively stable prior to each saturating pulse. This was consistent across all fluorescence measurements used to calculate rETR and NPQ, as shown in the Fig. A2, appendices data.

Measurements were conducted in specific containers filled with a diluted culture from the PBR (dilution factor of 5), allowing the insertion of the submersible optical probe of the PAM fluorometer to be held perpendicularly. Measurements were done on dark-acclimated samples, after 30 minutes of dark acclimatation. To minimize ambient light disturbances, the setup was placed in a shaded room where all measurements were taken. All measurements were done in duplicate per PBR before (at day 0) and during UV treatment, after 1, 3, 6, 8 and 10 days of exposure for Fv/Fm and RLC, and after 2 and 10 days of exposure, for OJIP and NPQ.

- The maximum quantum efficiency of PSII

Fv/Fm was measured, with a saturating pulse at 3 000 $\mu\text{mol photons m}^{-2} \text{s}^{-1}$, according to the equation [32]:

$$\frac{Fv}{Fm} = \frac{Fm - F0}{Fm}$$

With Fv the variable fluorescence, Fm the maximum fluorescence and F0 the minimum fluorescence yield (dark-acclimated minimum fluorescence yield).

- Fluorescence transients

The OJIP test represents the polyphasic fluorescence transients measured during the exposure of the culture to saturating light intensity. It corresponds to the different phases of reduction of the PSII electron acceptor, the quinones A and B (Q_A and Q_B) [43]. In the O phase, all photosynthetic reaction centres (RCs) are in a relaxed state, and Q_A and Q_B are in an oxidized state. The J phase is reached when

practically all primary acceptors, Q_A , have been reduced (Q_A^-). Then, when Q_B are reduced (Q_B^-), the I phase is reached. Finally, the P phase corresponds to the reduction of the plastoquinone (PQ) pool. The JIP test by Strasser *et al.* [54] was applied to translate experimental data into biophysical parameters: (1) ABS/RC, TR₀/RC, DI₀/RC and ET₀/RC that quantify the specific energy fluxes per RC and (2) M_0 , ψ_0 , ϕ_{D_0} , ϕ_{E_0} and Pi-ABS that quantify the quantum yield of primary photochemistry (Table 1).

Table 1. Definitions of OJIP parameters, based on Strasser *et al.* [43], measured in the dark-acclimated state. A reaction center (RC) is considered open when Q_A is in its oxidative state, conversely RC closes up when Q_A is reduced into Q_A^- . Q_A : primary quinone acceptor ; Q_B : secondary quinone acceptor ; PQ : plastoquinone ; PC : plastocyanin ; Cyt b6f : cytochrome b6f ; PSII : photosystem II :

OJIP Parameters	Definition	Formulas	Interpretation
<i>Specific fluxes</i>			
ABS/RC	Absorption flux of photons at the PSII antenna per active RC	$M_0 \times (1/V_i) \times (1/\phi_{P_0})$	The apparent antenna size
TR ₀ /RC	Maximum specific trapping flux	$M_0 \times (1/V_i)$	The rate, at time 0, by which an exciton is trapped in RC resulting in the reduction of Q_A to Q_A^-
ET ₀ /RC	Electron transport flux per RC at time 0	$M_0 \times (1/V_i) \times \psi_{E_0}$	The rate, at time 0, by which an electron moves beyond Q_A^- , resulting in a CO ₂ fixation
DI ₀ /RC	Dissipated energy flux per RC at time 0	$(ABS/RC) - (TR_0/RC)$	
<i>Quantum yield or efficiency</i>			
M_0	Slope at the origin of fluorescence rise (O-J)		The net rate of RC closure corresponding to Q_A reduction
ϕ_{P_0}	Maximum quantum yield of primary photochemistry	$TR_0/ABS = (1-F_0)/F_M$	The probability (at time 0) that an absorbed photon will be trapped into the PSII.
ψ_0	Maximum quantum yield of electron transport	ET_0/TR_0	The probability (at time 0) that a trapped exciton goes beyond Q_A^- in the electron transport chain.
ϕ_{E_0}	Quantum yield for electron transport at time 0	ET_0/ABS	The probability that an absorbed photon leads to the transport of an electron into the transport chain
ϕ_{D_0}	Quantum yield (at time 0) of energy dissipation	$1 - \phi_{P_0}$	
<i>Performance index</i>			
Pi-ABS	Index for energy conservation from photons absorbed by PSII until the reduction of intersystem electron acceptors	$(RC/ABS) \times (\phi_{P_0}/1 - \phi_{P_0}) \times (\psi_0/1 - \psi_0)$	The probability that an electron moves from PSII to PQ pool

- Rapid light curves

Rapid light curves were acquired through successive measurements of the culture exposed to increasing light intensity [44]. Thus, RLCs were performed with seven incremental irradiance steps (10; 20; 50; 100; 300; 500 and 1000 $\mu\text{mol photons m}^{-2} \text{s}^{-1}$) of 60 seconds. Then, physiological parameters ($rETR_m$, α , and E_k) were estimated by fitting the model developed by Platt *et al.* [55] to the experimental data:

$$rETR(I) = rETR_m \times \left(1 - e^{\left(-\alpha \times \frac{I}{rETR_m}\right)}\right)$$

With $rETR$ (AU) the relative electron transport rate (through PSII), $rETR_m$, the maximum relative electron transport rate, α the initial slope of the RLC at limiting irradiance.

$$E_k = \frac{rETR_m}{\alpha}$$

With E_k , the light saturation index in $\mu\text{mol photons m}^{-2} \text{s}^{-1}$.

NPQ induced by the RLC was calculated according to the Stern-Volmer NPQ [56,57] and following the equation:

$$NPQ_{induc} = \frac{F_m - F_m'}{F_m'}$$

With F_m the maximum fluorescence yield and F_m' the maximum fluorescent yield in actinic light measured at the final step.

- Non-photochemical quenching

Finally, NPQ allows the assessments of the photo-regulation capacity and the photosynthetic recovery of culture RCs. The microalga was exposed to continuous actinic light illumination (60 seconds at 1000 $\mu\text{mol photons m}^{-2} \text{s}^{-1}$) with five successive light pulses at saturating light (3 000 $\mu\text{mol photons m}^{-2} \text{s}^{-1}$) followed by a dark recovery phase (88 seconds) with three successive saturating light pulses.

2.6. Antioxidant analysis

2.6.1. Sampling and Extraction

At day 0, 2 and 10, approximately 500 mL of culture was centrifuged for 10 min at 4 500 g at 4°C. The supernatant was discharged, and the biomass was carefully collected, lyophilized, and stored at - 80°C. Then extraction step was conducted on freeze-dried biomass of each sample in a shaded room to prevent the degradation of photosensitive molecules. First, the biomass was suspended in methanol/dichloromethane (50:50 v/v) mixture (to facilitate the extraction of a broad spectrum of molecules) and sonicated in an ice bath for 10 minutes. Then, the extracts were filtered (Whatman GF/F 47mm), and this process was repeated until the biomass became colourless. Finally, the extracts were pooled, dried, and stored at -80°C until analysis.

2.6.2. TBARS assay

The TBARS (Thiobarbituric Acid Reactive Substance) assay measures antioxidant capacity to inhibit lipid peroxidation. This assay was previously found to be the best method to assess *Tetraselmis* antioxidant capacity [35]. The method in Coulombier *et al.* [35] was applied. An emulsion of linoleic acid (250 µL) with Tween 20 and phosphate buffer (20 mM, pH 7.4) was done and homogenized by sonication. A range of microalgae extract (200, 100, 50, 25, 12.5, 1.25 µg mL⁻¹) was done. Then, phosphate buffer (600 µL), FeSO₄ (200 µL, 0.01%), ascorbic acid (200 µL, 0.01%), extract solution or ethanol (as a blank) or Trolox at 200 µg/mL (as a positive control) (500 µL) and linoleic acid emulsion (500 µL) were successively added to Eppendorf tubes, mixed, and kept at 37°C for 24 hours in the dark. To stop the reaction, 400 µL of the reaction solution was mixed with butylated hydroxytoluene (BHT) (40 µL, 0.4%) and then with 440 µL of a mixture of thiobarbituric acid (TBA, 0.8 %) and trichloroacetic acid (TCA, 4 %). The solutions were incubated at 100°C for 30 minutes, cooled and centrifuged for 10 minutes at 10 000 g at 20°C. Then, the supernatant was measured at 534 nm. The half inhibition concentration (IC₅₀) values were obtained by plotting the percentage inhibition of linoleic acid peroxidation against their corresponding extract concentrations and drawing the regression lines. The IC₅₀ measures the

effectiveness of the algae in inhibiting a specific biological or biochemical function, in this case, lipid peroxidation. Thus, a lower IC_{50} value indicates a better inhibitor, as it requires a lower concentration to achieve the same level of inhibition.

2.7. Pigment analyses

To determine the pigment profile, 10 mL of the culture was centrifuged at day 0, 2 and 10 (10 min at 4500 g at 4°C), the supernatant was discarded and the pellet was frozen in liquid nitrogen and stored at -80°C. Then, pigments were extracted in relative darkness with 0.5 mL of solvent composed of 95 % of methanol (MeOH/H₂O v/v) with 2% of ammonium acetate and an internal standard (trans- β -Apo-8'-carotenal from Sigma Aldrich at 1 mg L⁻¹). Each sample was sonicated for 15 minutes in an ice bath and placed at -20°C for 20 minutes. Then it was centrifuged for 10 minutes (15 000 g, 5°C). The supernatant was discharged, and the pellet was kept and resuspended in 0.5 mL of the same solvent with a small glass putter. This process was repeated four times until the supernatant became colourless. Pigment analyses were done by high-pressure liquid chromatography (UHPLC-UV-DAD, Thermo Scientific, Vanquish) adapting the methods from Van Heukelem and Thomas [58].

Briefly, HPLC was conducted using Hypersil-Gold C18 (50×2 mm (i.d.), 2 μ m) silica-based reversed phase columns (Thermo Scientific). The Injection volumes were 2 μ L. The A and B mobile phases were a solution of MeOH/water (80:20, v/v) containing 1 M ammonium acetate and 0.05 % formic acid, and a solution of MeOH/Acetone (60:40, v/v) containing 0.05 % formic acid, respectively. The Hypersil Gold C18 column was eluted with a flow rate of 0.5 mL min⁻¹ using the following gradient: starting with 20% B, rising to 100% B at 6 min, held for 2 min, decreasing to 20% B over 0.5 min, and held for 2.5 min until the next run. Pigments were identified by their absorption spectra between 350 and 800 nm, measured with the photodiode-array detector (Thermo Scientific, Vanquish). Quantification (pg cell⁻¹), was performed at 450 nm by comparison with pigments standards (DHI, Denmark). Results are presented for major *Tetraselmis* pigments, in the order of elution: 9-cis-neoxanthine, violaxanthine, antheraxanthine, zeaxanthine, luteine, chlorophyll *a* (Chl *a*), *b* (Chl *b*), and β -carotene. All pigments are

expressed in $\mu\text{g cell}^{-1}$ and pigment ratios are expressed in g g^{-1} , to characterise the variation of the main pigment groups (chlorophylls and carotenoids).

2.8. Statistical analyses

All analyses were performed with R version 4.1.3 (2022-03-10). Statistical differences were tested using either one-way ANOVA or Kruskal-Wallis test when the conditions for application (homoscedasticity and/or normality hypotheses) were not met. *Post hoc* tests, specifically pairwise t-test or Dunn test, were used to compare paired days of exposure when necessary. For NPQ, a two-way repeated measures analysis was used to assess the significant differences between exposure times and time points generated by repeated the NPQ measurements during the NPQ induction by actinic light and the dark recovery period. Statistical significance was determined at a 95% of confidence level ($p\text{-value} < 0.050$).

3. Results

3.1 Growth performances and Elemental analysis

Throughout the experiment, cell concentration and light absorbance displayed a similar pattern. Both parameters showed a slight decrease (33% and 13%, respectively) after the addition of UV-A radiation from day 0 to day 2 (Table 2). Then, cultures returned to their initial state (*i.e.* day 0, before the UV-A addition). However, these variations in algal biomass were not statistically significant (Table 2, one-way ANOVA, cell concentration $F\text{-value} = 1.31$, $p\text{-value} = 0.30$ and light absorbance $F\text{-value} = 0.23$, $p\text{-value} = 0.96$).

Similarly, the cellular nitrogen content (QN) and the C:N ratio did not exhibit significant differences throughout the experiment (Table 2). The QN oscillated between $0.53 \pm 0.13 \text{ pmol cell}^{-1}$ and $0.89 \pm 0.020 \text{ pmol cell}^{-1}$. In contrast, the cellular carbon content (QC) was significantly affected by the UV-A exposure and ranged between $3.24 \pm 0.70 \text{ pmol cell}^{-1}$ and $5.44 \pm 0.21 \text{ pmol cell}^{-1}$, with a significant increase from day 0 to day 2 (Pairwise t-test $p\text{-value} = 0.044$).

Table 2. Cell concentration in $\times 10^6$ cell mL^{-1} , absorbance at 680 nm, carbon and nitrogen cell quota (QN and QC, in pmol cell^{-1}) and Carbon:Nitrogen (C:N) ratio of *Tetraselmis* sp. grown in continuous culture in PBR at different exposure times to UV-A radiation (0, 2 and 10 days). Data are expressed as mean \pm standard deviation. Statistical tests used were either one-way ANOVAs or Kruskal- Wallis test (*). Differences were considered significant at p -value < 0.050 (bolded value), different letters indicate significant differences between exposure times (from the post hoc test of ANOVA, pairwise t test).

Time exposure to UV-A (days)	0	1	2	3	4	8	9	10	<i>F</i> -value	<i>p</i> -value
Cell concentration in $\times 10^6$ cell mL^{-1}	3.51 \pm 0.69	3.16 \pm 0.056	2.70 \pm 0.42	3.26 \pm 0.20	3.46 \pm 0.20	3.010 \pm 0.042	2.90 \pm 0.34	3.36 \pm 1.19	1.31	0.30
Absorbance at 680 nm	0.71	0.63	0.62	0.67	0.75	0.69	0.68	0.67	0.23	0.96
Time exposure to UV-A (days)	0		2		10		<i>F</i> -value	<i>p</i> -value		
QN* (pmol cell^{-1})	0.53 \pm 0.13		0.89 \pm 0.020		0.76 \pm 0.20			0.11		
QC (pmol cell^{-1})	3.24 \pm 0.70 ^a		5.44 \pm 0.21 ^b		4.68 \pm 1.22 ^{ab}		7.48	0.012		
C:N* (mol mol^{-1})	6.17 \pm 0.30		6.080 \pm 0.16		6.16 \pm 0.15			0.67		

3.2 Pigment content

The pigment profile of *Tetraselmis* was assessed at different time of exposure to UV-A radiation and was composed of 9-cis-neoxanthin, violaxanthin, antheraxanthin, zeaxanthin, lutein, chlorophyll *a* (Chl *a*) and *b* (Chl *b*), and β -carotene. Total pigment content was influenced by the time of exposure to UV-A (Fig. 1a, one-way ANOVA, *F*-value = 5.71, *p*-value = 0.025). A significant increase was observed from day 0 (3.43 ± 0.91 pg cell^{-1}), to day 2 (5.43 ± 0.91 pg cell^{-1}) (Pairwise t-test *p*-value = 0.038). Then, a decrease in total pigment content, returning to the initial value, was observed from day 2 to 10, with values of 5.43 ± 0.91 pg cell^{-1} and 3.69 ± 0.84 pg cell^{-1} , respectively (Pairwise t test *p*-value = 0.049). Looking at the pigment ratios (Fig. 1b), no significant difference in the ratio of Chl *a* / Chl *b* was observed over time (one-way ANOVA, *F*-value = 3.17, *p*-value = 0.091). In contrary, there was a change in the ratio of total carotenoids / Chl *a* (one-way ANOVA, *F*-value = 6.091, *p*-value = 0.021). A significant decrease from day 0 (0.22 ± 0.017), to day 2 (0.19 ± 0.017) was observed (Pairwise t test *p*-value = 0.022). Similarly, a significant difference over time was observed for two carotenoids (mix

lutein + zeaxanthin and violaxanthin) regarding the variation in carotenoids over the total carotenoids (Fig 1c) (Kruskal Wallis test, respectively p -value = 0.021 and p -value = 0.012). In fact, a significant increase from day 0 to day 2 was present for the mix lutein + zeaxanthin (Dunn test p -value = 0.024) and a significant decrease was observed for violaxanthin from day 0 to day 2 (Dunn test p -value = 0.0098). For the other carotenoids, no significant difference was observed over the time of exposure to UV-A.

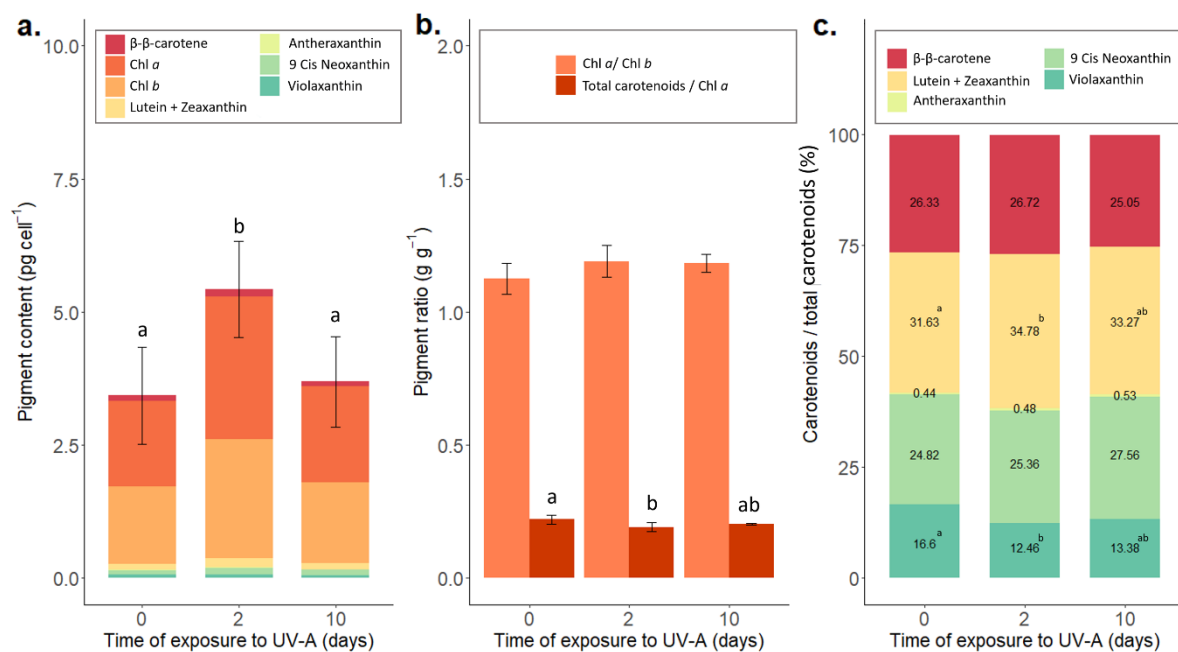


Fig. 1. Pigment profile and content in pg cell^{-1} (a), pigment ratios (chl a / chl b and total carotenoids / chl a) (b) and percentage of carotenoids (carotenoids / total carotenoids) (c) of *Tetraselmis sp.* in continuous cultures exposed to UV-A (at different times of exposure 0, 2 and 10 days). Pigments are β β -carotene, chlorophyll a (Chl a), chlorophyll b (Chl b), lutein, zeaxanthin, antheraxanthin, 9-Cis-Neoxanthin, and violaxanthin. Data expressed as mean \pm standard deviation. Differences were considered significant at p -value < 0.050. Different letters indicate a significant difference between time of exposure to UV-A.

3.3 Antioxidant capacity

The antioxidant activities (IC_{50} values) measured using the TBARS assay are shown in Fig 2. Before and during the UV-A exposure, the culture showed relatively low IC_{50} values, which highlight an anti-lipid

peroxidation activity of the algal extracts. The IC_{50} ranged between $2.87 \mu\text{g mL}^{-1}$ and $19.57 \mu\text{g mL}^{-1}$. However, the best value (*i.e.*, the lowest IC_{50} value) was measured at day 0 ($2.87 \pm 0.24 \mu\text{g mL}^{-1}$), before the addition of UV-A radiation. Then, significant differences were observed between the times of exposure to UV-A (one-way ANOVA, p -value = 0.017); after ten days of UV-A exposure, the IC_{50} significantly increase by a factor 7 (*i.e.* the antioxidant capacity decrease) compared to the initial value at day 0 (Fig 2., Pairwise t test, p -value = 0.015).

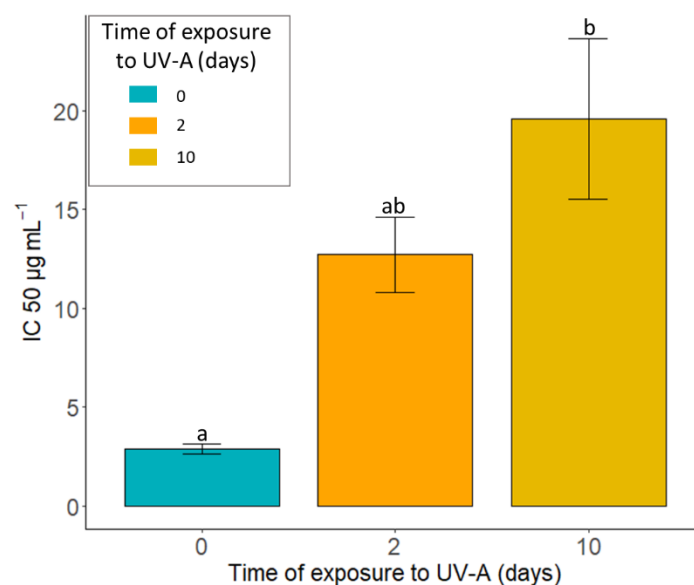


Fig. 2. Antioxidant capacity (IC_{50} , $\mu\text{g mL}^{-1}$) of *Tetraselmis* sp. in continuous cultures exposed to UV- A stress (at different times of exposure: 0, 2 and 10 days). Antioxidant capacity of reference compounds Trolox ($IC_{50} = 0.15 \mu\text{g mL}^{-1}$) and α - tocopherol ($IC_{50} = 0.78 \mu\text{g mL}^{-1}$). Data expressed as mean \pm standard deviation. Differences were considered significant at p -value < 0.05. When letters differ, it indicates a significant difference between exposure times.

3.4 Maximum quantum efficiency of the PSII,

RLCs and NPQs measurements

The PSII maximum quantum yield (F_v/F_m) of *Tetraselmis* sp. was clearly affected by the UV-A exposure over time (Fig. 3a). *Tetraselmis* showed high initial F_v/F_m values before the addition of UV-A (0 day), around 0.64 (Fig. 3a). However, a significant difference was observed following the addition of UV-A

(one-way ANOVA, p -value < 0.001). A significant lower Fv/Fm value, around 0.55, was reached after the third day of UV-A exposure (Fig. 3a, results of the Pairwise t-test in Table A2 in the Appendices data). This decrease from 0.64 ± 0.01 to 0.55 ± 0.05 (14%) was followed by a gradual increase until the end of the experiment, where the initial Fv/Fm was recovered (0.65 ± 0.01) by Day 10.

Using the parameters extracted from the RLCs (Fig. 3b, Fig. 4), significant differences were observed over time owing to the addition of UV-A radiation. The kinetic of rETR as function of PAR, used here as a proxy for photosynthetic activity, was modified by the addition of UV-A radiation. First, no photoinhibition was observed under all tested conditions. However, differences were observed over time, with the highest values of rETR found after one day of exposure, and the lowest one before the addition of UV-A (day 0) and after 6 and 8 days of exposure to UV-A radiation (Fig. 3b). Regarding the other parameters extracted from the RLCs (rETRm, alpha, Ek, NPQind, Fig. 4), the maximum electron transport rate (rETRm) and the light saturation coefficient (Ek) showed a similar tendency and significant variations were found over time following UV-A exposure (Fig. 4, and table 3). They both increased after the addition of UV-A radiation, which was significant for rETRm (from day 0, 34.80 ± 3.12 , to day 1, 43.99 ± 5.43 , Pairwise t-test, rETRm p -value = 0.022). It was followed by a significant decrease, in both parameters, until day 6 of exposure (from day 1 to 6, Fig. 4 a and b, Pairwise t-test, rETRm p -value < 0.0010, Ek p -value < 0.0010) and then by an increase until the end of the experiment (from day 6 to 10, Pairwise t test, rETRm p -value = 0.011, Ek p -value = 0.033). Regarding the maximum light utilization coefficients (alpha), it fluctuated between 0.20 ± 0.010 and 0.22 ± 0.010 , with no significant differences detected (Fig. 4c). Finally, non-photochemical quenching induced by the RLCs (NPQind) varied from 1.37 ± 0.73 before the addition of UV-A to 0.54 ± 0.18 after three days of exposure, reaching its minimum value. No significant differences were found (table 3).

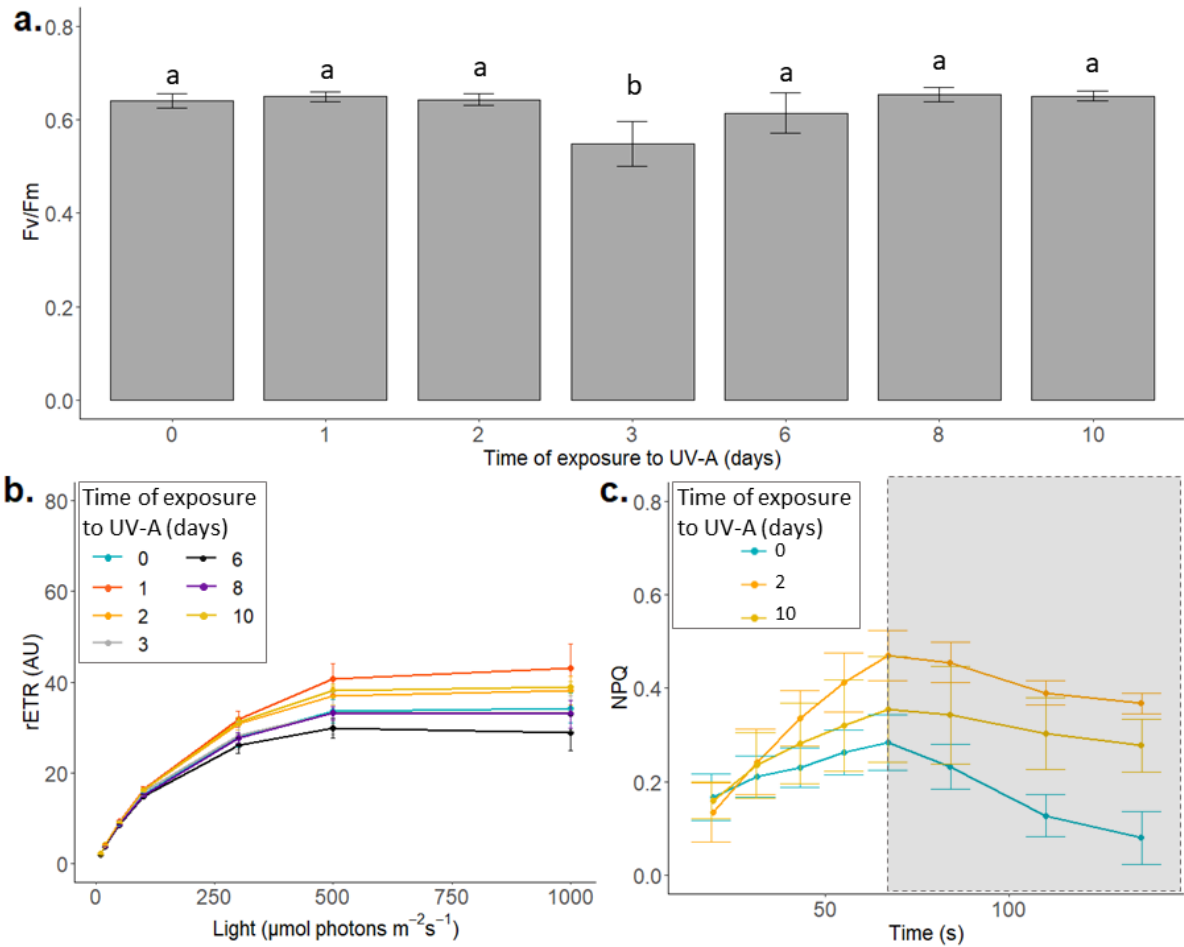


Fig. 3. a. Maximum quantum yield (Fv/Fm), **b.** Rapid light curves expressed as relative electron transport rate (rETR) as a function of photosynthetic active radiation (PAR) of dark incubated *Tetraselmis* sp. grown in continuous culture in PBR and exposed to UV-A treatment, from day 0 (before the treatment) to day 10 (10 days of treatment). **c.** Non-Photochemical Quenching (NPQ) over the induction (white background) and dark recovery (grey background) of *Tetraselmis* in continuous culture in PBR exposed to UV-A treatment, from day 0 (before the treatment) to day 10 (10 days of treatment). Data are expressed as mean \pm standard deviation.

In addition, regarding the NPQ recovery (Fig. 3c), algae exposed to UV-A showed a slower and incomplete recovery in contrast to the NPQ recovery observed on day 0, where the NPQ value returned to the initial value of the light/dark cycle. Finally, after 10 days of UV-A exposure, the actinic light induced a lower increased of NPQ over time, but the recovery remained slow and incomplete compared to day 0.

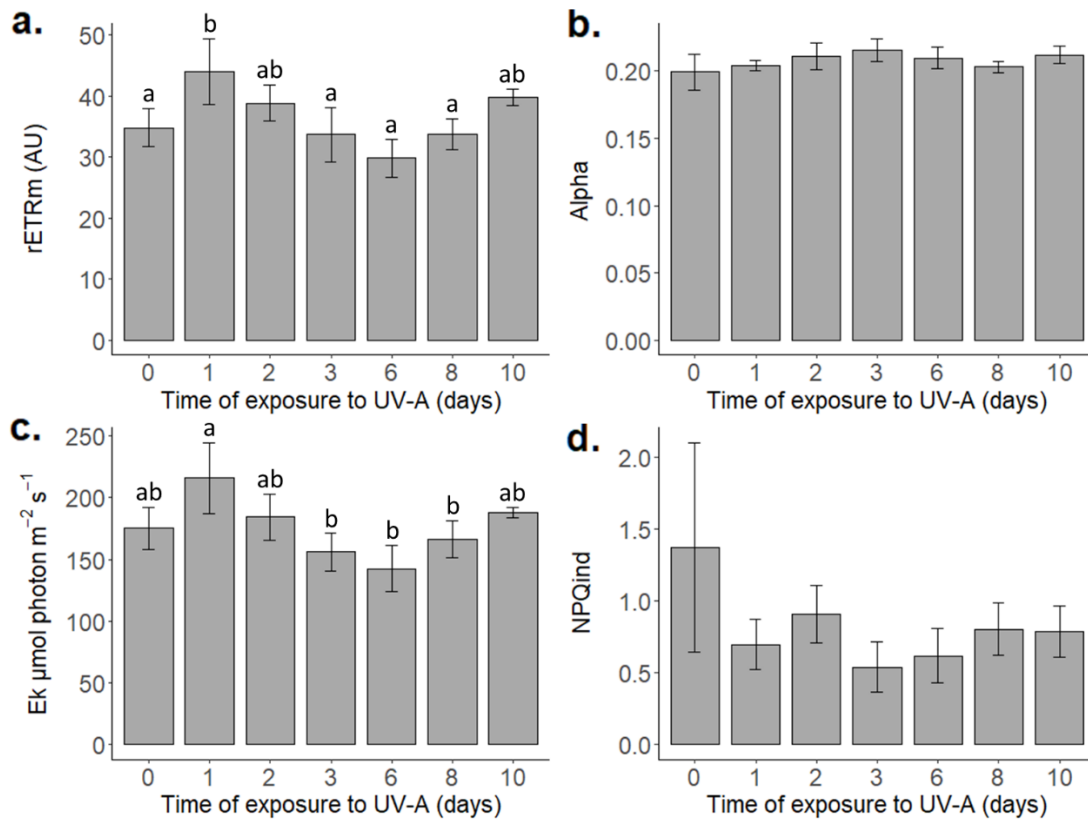


Fig. 4. Parameters obtained from rapid light curves carried out on dark-acclimated *Tetraselmis* sp. in continuous cultures, exposed to UV-A treatment. **a.** rETRm, the maximum relative electron transport rate in AU; **b.** Ek, the light half saturation coefficient in $\mu\text{mol photons m}^{-2} \text{s}^{-1}$; **c.** alpha, the maximum light utilization coefficient for PSII; and **d.** NPQind, the non-photochemical quenching induced by the RLC. Data are expressed as mean \pm standard deviation. Statistical tests used were either one-way ANOVAs or Kruskal-Wallis test (*). Differences were considered significant at $p < 0.050$ (bolded value), values with different letters indicate significant differences between exposure times (from post hoc tests pairwise t-test or Dunn test).

Table 3. Statistical values from the statistical tests, either one-way ANOVAs or Kruskal-Wallis test (*). Differences were considered significant at $p < 0.050$ (bolded value). The statistical analyses were implemented on parameters obtained from the rapid light curves carried out on dark-acclimated *Tetraselmis* sp. in continuous cultures, exposed to UV-A treatment with rETRm the maximum relative electron transport rate in AU; alpha, the maximum light utilization coefficient for PSII; Ek, the light half saturation coefficient in $\mu\text{mol photons m}^{-2} \text{s}^{-1}$; and NPQind, the non-photochemical quenching induced during the RLC.

Time exposure to UV-A (days)	<i>F</i> -value	<i>p</i> -value
rETRm	7.38	< 0.0010
Alpha	2.27	0.28
Ek	7.030	< 0.0010
NPQind*		0.056

3.5 Polyphasic chlorophyll *a* fluorescence transient (OJIP test)

To complement our previous results to assess the status of *Tetraselmis* PSII exposed to UV-A radiation, we examined the fast Chl *a* fluorescence transient. The “raw” and normalized Chl *a* fluorescence kinetics are depicted in Fig. 5. All curves showed a typical polyphasic trend, with a rise from O to P. The slope and the shape of the fluorescence transient represent the photophysiological state of the culture and the reduction state of the PSII acceptors. Regarding the “raw” Chl *a* fluorescence transient (Fig. 5a), the addition of UV-A radiation led to a decreased in the fluorescence intensities of the OJIP curves compared to day 0. This decrease was quickly observed after the addition of UV-A radiation. Indeed, at day 1, the intensity of the Chl *a* fluorescence decreased sharply, a tendency that continued until reaching the lowest values at day 3. However, the fluorescence intensity increased slightly from day 3 to the end of the experiment (day 10, Fig. 5a).

Considering that the intensity of F_0 was different during UV-A exposure, the OJIP curves were normalized at the O level F_0 , $f(t) = (F_t - F_0) / F_0$ (Fig. 5b). Differences in intensities were mainly observed

between day 0 (before UV-A radiation) and day 3 (after 3 days of UV-A radiation) while on days 1 and 10, the curves were more similar to day 0 (Fig. 5b).

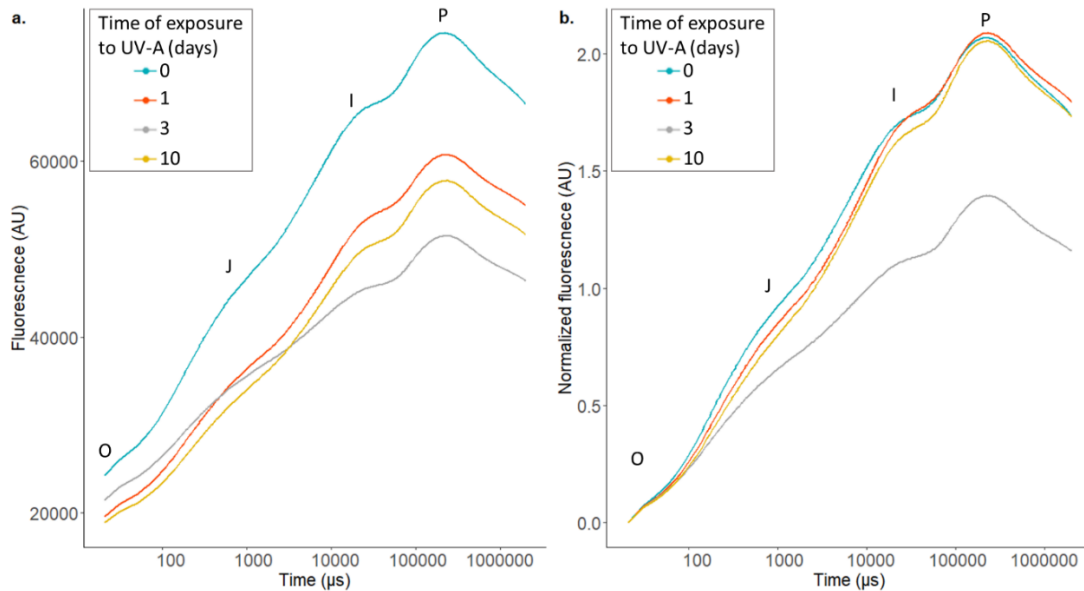


Fig. 5. Polyphasic fluorescence OJIP curves of *Tetraselmis* sp.. in continuous culture in PBR exposed to UV- A treatment, from t0 (before the treatment) to t10 (10 days of treatment), with the average fluorescence transients (a.) and normalized at F0 (b.)

Using these curves, eleven biophysical parameters were calculated from the OJIP test (Table 4). Statistical differences owing to the time of exposure to UV- A were observed for five parameters including the specific fluxes corresponding to the absorption flux of photons at the PSII antenna by active reaction center (ABS/RC) and the dissipated energy flux per RC at time 0 (DI_0/RC). In addition, variations were also observed in different quantum yields, namely the quantum yield for electron transport (ϕE_0), and the performance index for energy conservation from photons absorbed by PSII until the reduction of intersystem electron acceptors (PI Abs). Two different and logical trends were observed, differentiating specific fluxes and quantum yields. Parameters representing quantum yields and performances (ϕE_0 , PI Abs and F_v/F_m) decreased after short exposure to UV-A, with the lowest values recorded on day 3, while the specific fluxes increased (ABS/RC and DI_0/RC), reaching higher values at day 3 (Table 4). These variations (decrease and increase) were found significant (Table A3,

Appendices data). The other parameters, M_0 , ψ_0 , ϕ_{D0} , Tr_0/Rc and Et_0/Rc did not show any significant differences owing the addition of UV-A radiation.

Table 4. Photosynthetic parameters obtained from OJIP fluorescence transients on dark acclimated *Tetraselmis* sp. exposed to UV-A radiation in continuous cultures in PBR at different exposure times. Data are expressed as mean \pm standard deviation. Statistical tests used were either one-way ANOVAs or Kruskal-Wallis tests and post hoc tests (pairwise t-test or Dunn test) were undertaken (* corresponds to non-parametric tests). Differences were considered significant at $p < 0.050$ (bolded value), letters a and b indicate significant differences between exposure times. The quantum efficiency or flux ratios parameters: M_0 , approximate value of the initial slope of the curve at the origin of the fluorescence rise; ψE_0 The probability that a trapped photon can move an electron into the transport chain further than Q_A^- ; ϕE_0 , quantum yield of electron transport; ϕD_0 , quantum yield of energy dissipation; PI ABS, performance index; and the specific fluxes parameters : ABS/RC, absorption flux or effective antenna size of an active reaction center (RC); Tr_0/RC , maximal trapping rate of PSII, it is the trapped energy flux leading to a reduction of the primary acceptor; E_{t0}/RC , electron transport in an active RC; D_{i0}/RC , effective dissipation in an active RC.

Time exposure to UV-A (days)		0	1	3	10	<i>F-value</i>	<i>p-value</i>
Specific fluxes	ABS/RC	3.28 \pm 0.33 ^b	3.27 \pm 0.20 ^b	4.08 \pm 0.46 ^a	3.14 \pm 0.16 ^b	7.66	0.0040
	Tr_0/RC	2.10 \pm 0.25	2.12 \pm 0.10	2.22 \pm 0.17	2.04 \pm 0.070	0.87	0.49
	E_{t0}/RC	1.12 \pm 0.010	1.18 \pm 0.040	1.11 \pm 0.060	1.15 \pm 0.020	2.64	0.097
	D_{i0}/RC^*	1.18 \pm 0.090 ^{ab}	1.15 \pm 0.10 ^{ab}	1.86 \pm 0.37 ^a	1.10 \pm 0.090 ^b		0.023
Quantum yields and performance index	M_0	0.98 \pm 0.25	0.94 \pm 0.060	1.11 \pm 0.15	0.89 \pm 0.070	1.54	0.25
	ψE_0^*	0.64 \pm 0.070	0.65 \pm 0.010	0.64 \pm 0.030	0.65 \pm 0.020		0.066
	ϕE_0	0.35 \pm 0.040 ^b	0.36 \pm 0.010 ^b	0.28 \pm 0.040 ^a	0.37 \pm 0.020 ^b	8.75	0.002
	ϕD_0^*	0.36 \pm 0.010	0.35 \pm 0.010	0.45 \pm 0.050	0.35 \pm 0.010		0.87
	PI ABS	0.68 \pm 0.26 ^b	0.72 \pm 0.10 ^b	0.32 \pm 0.13 ^a	0.78 \pm 0.14 ^b	6.19	0.0090

4. Discussion

Microalgae from different geographical regions are exposed and adapted to different intensities of UV radiation. The UV intensities exhibit an inverse relationship with latitude, being highest in tropical regions and lowest in polar regions [59]. The genus *Tetraselmis* is found in a wide range of habitats [36]. In this study, the species of interest (*Tetraselmis* sp.) has been isolated in coastal waters of New Caledonia. This archipelago, located in the intertropical zone, is characterized by tropical weather, and high solar irradiance therefore high UV radiation [41].

4.1 *Growth performances, standard elemental stoichiometry, and pigment content*

Our results showed that the algal biomass of *Tetraselmis* sp. was not affected by the UV-A radiation. While a slight decrease was noticed after a few days of exposure (1-2 days), it was followed by a return to the initial state (*i.e.*, day 0 before the UV-A addition). In the literature, both positive and negative effects of UV-A exposure on microalgae growth have been reported. Similarly to the present study, results on *Dunaliella bardawil* growth suggested a quick acclimation phase to UV-A after 24h of exposure [27]. Döhler *et al*, [60] also reported that the growth of *Dunaliella tertiolecta* was negatively affected by short-time exposure to UV-A. However, in some studies, algal growth was enhanced after an adaptation to a long-term exposure to UV-A (e.g. *Nannochloropsis gaditana*, *Diplospira* sp., *Dunaliella bardawil*) [25,61–63].

Similarly, to cell concentration, the standard elemental stoichiometry was slightly affected by UV-A exposure. The standard elemental stoichiometry is generally assumed to be 106 C: 16 N: 1 P under nutrient-replete conditions [64] and is often used to assess nutrient limitation in marine phytoplankton [65–67]. Therefore, the C/N ratio for cells in good nutritional status is assumed to be close to 6.6 for species growing in nutrient replete conditions [68–70]. In this study, the objective was to maintain *Tetraselmis* in replete conditions, which was achieved, as the C/N ratio remained around 6.1 during all

the experiment. However, a small increase in the C cellular quota was noticed at day 2, suggesting a small positive short-term impact of UV-A on photosynthesis and C assimilation.

UV-A radiation can stimulate pigment accumulation. Previous studies have demonstrated that a proper ratio between PAR and UV-A induces the accumulation of carotenoids [25–27]. In this study, UV-A has an impact, leading to an increase in total pigment content, and a different pattern for carotenoid abundance was observed with a decrease in violaxanthin and an increase in zeaxanthin and lutein. Those carotenoids (xanthophylls) play a role in photoprotection through the xanthophyll cycle [71,72]. In conditions of high light energy, violaxanthin is transformed into zeaxanthin in order to neutralize oxidative stress [73]. Thus, the xanthophyll cycle could have shifted towards photoprotective mechanisms to counteract an oxidative stress.

4.2. Chlorophyll a fluorescence and antioxidant capacity

Similarly to cell concentration and to C cellular quota, the F_v/F_m , a proxy of the PSII health often used as an indicator of environmental stress [33,74,75], showed lower values following few days of exposure (3 days) to UV-A. However, this decrease was also followed by a return to the basal state (from day 3 to 10) suggesting an acclimation period of a few days. It confirms that UV-A induces a relative stress in the short-term on *Tetraselmis* particularly on the PSII. Previous studies showed that photosynthetic organisms might suffer from irreversible damage to important metabolic processes due to UV-A exposure [28,76–78]. However, our experimental design was constructed to prevent irreversible damage, exposing the algae to relatively low levels of UV-A to induce a stress response without causing major damages.

Rapid light curves (RLCs) are used to estimate photosynthetic parameters ($rETR_m$, E_k , α) providing information into the photosynthetic activity and photoacclimation state of the culture [79,80]. In this study, with the exception of α , parameters extracted from the RLCs, namely $rETR_m$ and E_k , showed a similar trend over time under UV-A exposure (Fig. 4, and Table 3). The maximum electron transport rate ($rETR_m$) and the light saturation coefficient (E_k) significantly increased over the first day of

exposure followed by a decrease until day 6, to finally return to values similar to the initial value on day 0 (at day 8 and 10). These variations observed until day six indicated an impact of UV-A exposure, with a gradual reduction of the PSII activity of *Tetraselmis*. However, the return to basal values highlights the resilience of this species to UV-A during long-term exposure. *Tetraselmis* first enhanced its photosynthetic capacity especially to use high light (day 1, higher rETR and Ek). Still, this capacity was quickly impacted by UV-A (day 1 to 6, decrease in rETRm and Ek) before a gradual acclimation of the PSII occurred in the end of the experiment from day 6 to 10. In contrast, alpha was not impacted during the experiment, indicating that the capacity of *Tetraselmis* to use “low light” intensity is scarcely impacted by UV-A in the present case.

Previous studies on the effect of UV exposure on higher plants have reported that UV-A can induce a degradation of (i) RC subunits of PSII, mainly affecting proteins D1 and D2, with a higher impact on protein D1 [77,81], (ii) binding sites of Q_A and Q_B [77], and (iii) the inactivation of the oxygen evolving complex (OEC) a donor side component of PSII, through the release of manganese ions from the OEC [77,82]. However, in the present study, a high renewal rate of 0.70 day⁻¹ and N-supplementation were implemented. It reduces the potential impact of N-limitation to solely assess the effect of UV rather than the combined effect of UV and N-limitation. In fact, N-limitation affects PSII efficiency by gradually decreasing photosynthetic pigments [83], PSII maximum quantum yield [75,84,85], and gradually inactivating protein D1 in PSII RC, owing to the reduced amount of N available to synthesize it.

To clarify and evaluate the impacts of UV-A on the photosynthetic structure and function, we also monitored the fast fluorescent chlorophyll *a* transient, through the OJIP test. Similarly, significant differences were highlighted after 3 days of exposure, confirming the impact of UV-A on PSII, particularly on the fluorescent transient kinetic and calculated parameters. Lower values were found for the performance index (PI ABS) and the quantum yield for electron transport at day 0 ($\phi E0$). The PI ABS represents a measure of the overall functionality of PSII photochemistry [86]. It is a sensitive indicator of environmental stress on photosynthesis [43,87]. Here, the results of PI ABS are in line with the Fv/Fm results showing the negative impact of UV-A on short term exposure (decrease after 3 days

of exposure). In addition, a lower value was noted for $\phi E0$ after 3 days of exposure, indicating a lower quantum yield efficiency of electron transport. These results highlight a disruption of the electron transport chain, mainly at the quinone acceptor binding sites (Q_A and Q_B). This is supported by previous studies on higher plants that reported the disruption of the electron transport at (i) the water oxidizing complex and (ii) quinone acceptor binding sites (mainly Q_B and Q_A) due to UV-A radiation [28,77,78,81]. This is consistent with the higher value found at day 3 of exposure for ABS/RC, indicating an effect of UV-A on the absorption of photons at the antenna per active RC. It could be explained by a decrease or degradation in active RC induced by UV-A, along with the concomitant ROS production. Indeed, ROS may degrade RC subunits of PSII (*i.e.*, proteins D1 and D2). Similarly, a higher value was found at day 3 for $D1_o/RC$, suggesting cellular modifications related to photoprotective mechanisms, although $\phi D0$ and NPQ_{ind} remained stable. Thus, to clarify this, we followed the photo-regulation capacity and photosynthetic recovery of culture RCs during continuous exposure to actinic light followed by a dark recovery period. Microalgae modulate their NPQ by dissipating the energy as heat to cope with an excess of energy induced by high or fluctuating light and to prevent long-lasting damage of the photosynthetic apparatus [88–90]. Results from the NPQ induction period showed that higher NPQ values were reached when the culture was exposed to UV-A radiation. UV-A exposure induced a higher photoprotective response when *Tetraselmis* was exposed to the actinic light by promoting the heat dissipation. Ponte *et al.*, [91], have observed a similar NPQ response previously on the higher plant *Solanum lycopersicum* L. (tomato) under low doses of UV-A. Additionally, it also reduced the NPQ recovery capacity, as incomplete recovery during the dark period was observed suggesting a potential NPQ exhaustion leading to irreversible NPQ. Reduced NPQ efficiency and recovery might induce damages to D1 proteins, decline in the photosynthetic efficiency, chronic photoinhibition and/or ROS production [92]. As no photoinhibition was observed during the experiment, another photoprotective mechanism, such as antioxidant, could be involved in controlling and neutralizing ROS before any permanent damage occurred.

The results from the TBARS assay showed a significant effect of UV-A exposure on the antioxidant capacity of *Tetraselmis*, with an increase of IC₅₀ values over time exposure. This increase can be attributed to the utilization or degradation of antioxidant molecules by the organism to counteract an increased production of ROS [93,94]. Microalgae produce a wide range of molecules which play an important role in the antioxidant response such as carotenoids, fatty acids, vitamins, or other metabolites [5–7,10]. This defence mechanism is involved in the regulation of ROS [95–97] which are radical forms of oxygen produced by all aerobic organisms. As by-products of photosynthesis, ROS production affects the activity of and to a greater extend, overall photosynthesis [96,98–100].

4.2 Implication for the production of extract with high antioxidant capacity

In the present study, reference compounds Trolox (0.15µg mL⁻¹) and α-tocopherol (0.78µg mL⁻¹) obtained the best IC₅₀. Nevertheless, culture before the UV-A treatment showed an IC₅₀ of 2.87 ± 0.24 µg mL⁻¹, which is close and in the same order of magnitude as the reference compounds. This result, under optimal (*i.e.*, no stress) growth condition, represents a 5.38-fold improvement over findings by Coulombier *et al.*, 2020 [35] and a 1.20-fold enhancement over Coulombier *et al.*, 2020 [20]. In addition, it confirms that the addition of a stress, as highlighted in [35] or N-limitation or acidic condition, as outlined in Coulombier *et al.*, 2021 [20] reduces the antioxidant capacity of *Tetraselmis* sp..

5. Conclusion

This study aimed to characterize the response of *Tetraselmis* sp. to UV-A stress. To sum up, a negative effect on the photosynthetic efficiency was observed after short-term exposure to UV-A, which can be linked to a decrease in the electron transport efficiency. This decrease was followed by a potential adaptation of the photochemistry over time to UV-A exposure since a return to the initial state was observed. However, UV-A exposure also influenced antioxidant capacity, by inducing a decrease in

antioxidant capacity (indicated by an increase in IC_{50}) linked to the use of antioxidant compounds. While a strong antioxidant capacity was observed before the exposure to UV-A, confirming the potential of *Tetraselmis* sp. for antioxidant production, we discourage the use of UV-A to enhance antioxidant capacity in *Tetraselmis*.

Declaration of competing interest

The authors declare that they have no known competing financial interests or personal relationships that could have appeared to influence the work reported in this paper.

CRedit authorship contribution statement

Anna Isaia: Writing – review & editing, Writing – original draft, Formal analysis, Data curation, Conceptualization. **Noémie Coulombier:** Writing – review & editing, Supervision, Formal analysis, Data curation, Conceptualization. **Loïc Le Dean:** Writing – review & editing, Supervision, Project administration, Funding acquisition, Conceptualization. **Vincent Meriot:** Writing – review & editing, Formal analysis. **Thierry Jauffrais:** Writing – review & editing, Writing – original draft, Supervision, Project administration, Funding acquisition, Formal analysis, Data curation, Conceptualization.

Data availability

The authors declare that all data supporting the findings of this study are available within the paper and its supplementary file.

Acknowledgments

The authors acknowledge the Province Nord, the Province Sud, the Government of New Caledonia, and the Comité Interministériel de l'Outre-Mer (CIOM) for financial support through the Aquaculture

of Microalgae in New Caledonie (AMICAL) 1 and 2 research programs. The South Province of New Caledonia (n°26960, n°1546 and n°9705) and the North Province of New Caledonia (n°609011-55 and n°609011-54) delivered the sampling authorizations. We would like also to acknowledge Ifremer for financing the Master 2 thesis of Anna Isaia. We would like to thank Anne Desnues from the LAMA (Laboratoire des Moyens Analytiques, IRD, Noumea) for the elemental analyses.

References

- [1] A.-L. Groussin, S. Antoniotti, Valuable chemicals by the enzymatic modification of molecules of natural origin: Terpenoids, steroids, phenolics and related compounds, *Bioresource Technology* 115 (2012) 237–243. <https://doi.org/10.1016/j.biortech.2011.10.050>.
- [2] S.C. Lourenço, M. Moldão-Martins, V.D. Alves, Antioxidants of Natural Plant Origins: From Sources to Food Industry Applications, *Molecules* 24 (2019) 4132. <https://doi.org/10.3390/molecules24224132>.
- [3] W. Fu, D.R. Nelson, Z. Yi, M. Xu, B. Khraiweh, K. Jijakli, A. Chaiboonchoe, A. Alzahmi, D. Al-Khairi, S. Brynjolfsson, K. Salehi-Ashtiani, Bioactive Compounds From Microalgae: Current Development and Prospects, in: *Studies in Natural Products Chemistry*, Elsevier, 2017: pp. 199–225. <https://doi.org/10.1016/B978-0-444-63929-5.00006-1>.
- [4] Ç. Yarkent, C. Gürlek, S.S. Oncel, Potential of microalgal compounds in trending natural cosmetics: A review, *Sustainable Chemistry and Pharmacy* 17 (2020) 100304. <https://doi.org/10.1016/j.scp.2020.100304>.
- [5] K.H.M. Cardozo, T. Guaratini, M.P. Barros, V.R. Falcão, A.P. Tonon, N.P. Lopes, S. Campos, M.A. Torres, A.O. Souza, P. Colepicolo, E. Pinto, Metabolites from algae with economical impact, *Comparative Biochemistry and Physiology Part C: Toxicology & Pharmacology* 146 (2007) 60–78. <https://doi.org/10.1016/j.cbpc.2006.05.007>.
- [6] D. Kelman, E.K. Posner, K.J. McDermid, N.K. Tabandera, P.R. Wright, A.D. Wright, Antioxidant Activity of Hawaiian Marine Algae, *Marine Drugs* 10 (2012) 403–416. <https://doi.org/10.3390/md10020403>.
- [7] C. Paliwal, M. Mitra, K. Bhayani, S.V.V. Bharadwaj, T. Ghosh, S. Dubey, S. Mishra, Abiotic stresses as tools for metabolites in microalgae, *Bioresource Technology* 244 (2017) 1216–1226. <https://doi.org/10.1016/j.biortech.2017.05.058>.
- [8] M.F.G. Assunção, R. Amaral, C.B. Martins, J.D. Ferreira, S. Ressurreição, S.D. Santos, J.M.T.B. Varejão, L.M.A. Santos, Screening microalgae as potential sources of antioxidants, *J Appl Phycol* 29 (2017) 865–877. <https://doi.org/10.1007/s10811-016-0980-7>.
- [9] M.H. Bule, I. Ahmed, F. Maqbool, M. Bilal, H.M.N. Iqbal, Microalgae as a source of high-value bioactive compounds, *Front Biosci* 10 (2018) 197–216. <https://doi.org/10.2741/s509>.
- [10] N. Coulombier, T. Jauffrais, N. Lebouvier, Antioxidant Compounds from Microalgae: A Review, *Marine Drugs* 19 (2021) 549. <https://doi.org/10.3390/md19100549>.
- [11] L. Gouveia, A.E. Marques, J.M. Sousa, P. Moura, N.M. Bandarra, Microalgae – source of natural bioactive molecules as functional ingredients, *Food Science & Technology Bulletin: Functional Foods* 7 (2010) 21–37. <https://doi.org/10.1616/1476-2137.15884>.
- [12] S. Singh, B.N. Kate, U.C. Banerjee, Bioactive Compounds from Cyanobacteria and Microalgae: An Overview, *Critical Reviews in Biotechnology* 25 (2005) 73–95. <https://doi.org/10.1080/07388550500248498>.

- [13] B.D.S. Vaz, J.B. Moreira, M.G.D. Morais, J.A.V. Costa, Microalgae as a new source of bioactive compounds in food supplements, *Current Opinion in Food Science* 7 (2016) 73–77. <https://doi.org/10.1016/j.cofs.2015.12.006>.
- [14] B. Austin, E. Baudet, M. Stobie, Inhibition of bacterial fish pathogens by *Tetraselmis suecica*, *J Fish Diseases* 15 (1992) 55–61. <https://doi.org/10.1111/j.1365-2761.1992.tb00636.x>.
- [15] A.W. Farahin, F.M. Yusoff, M. Basri, N. Nagao, M. Shariff, Use of microalgae: *Tetraselmis tetrathele* extract in formulation of nanoemulsions for cosmeceutical application, *J Appl Phycol* 31 (2019) 1743–1752. <https://doi.org/10.1007/s10811-018-1694-9>.
- [16] G.A.O. Moser, J.J. Barrera-Alba, M.J. Ortega, C. Alves-de-Souza, A. Bartual, Comparative characterization of three *Tetraselmis chui* (Chlorophyta) strains as sources of nutraceuticals, *J Appl Phycol* 34 (2022) 821–835. <https://doi.org/10.1007/s10811-021-02675-x>.
- [17] S. Choudhury, P. Panda, L. Sahoo, S.K. Panda, Reactive oxygen species signaling in plants under abiotic stress, *Plant Signaling & Behavior* 8 (2013) e23681. <https://doi.org/10.4161/psb.23681>.
- [18] P. Sharma, A.B. Jha, R.S. Dubey, M. Pessarakli, Reactive Oxygen Species, Oxidative Damage, and Antioxidative Defense Mechanism in Plants under Stressful Conditions, *Journal of Botany* 2012 (2012) 1–26. <https://doi.org/10.1155/2012/217037>.
- [19] F. Ahmed, K. Fanning, M. Netzel, P.M. Schenk, Induced carotenoid accumulation in *Dunaliella salina* and *Tetraselmis suecica* by plant hormones and UV-C radiation, *Appl Microbiol Biotechnol* 99 (2015) 9407–9416. <https://doi.org/10.1007/s00253-015-6792-x>.
- [20] N. Coulombier, P. Blanchier, L. Le Dean, V. Barthelemy, N. Lebouvier, T. Jauffrais, The effects of CO₂-induced acidification on *Tetraselmis* biomass production, photophysiology and antioxidant activity: A comparison using batch and continuous culture, *Journal of Biotechnology* 325 (2021) 312–324. <https://doi.org/10.1016/j.jbiotec.2020.10.005>.
- [21] B. Gao, J. Hong, J. Chen, H. Zhang, R. Hu, C. Zhang, The growth, lipid accumulation and adaptation mechanism in response to variation of temperature and nitrogen supply in psychrotrophic filamentous microalga *Xanthonema hormidioides* (Xanthophyceae), *Biotechnol Biofuels* 16 (2023) 12. <https://doi.org/10.1186/s13068-022-02249-0>.
- [22] A.C. Guedes, H.M. Amaro, R.D. Pereira, F.X. Malcata, Effects of temperature and pH on growth and antioxidant content of the microalga *Scenedesmus obliquus*, *Biotechnol Progress* 27 (2011) 1218–1224. <https://doi.org/10.1002/btpr.649>.
- [23] M.F. Pessoa, Harmful effects of UV radiation in Algae and aquatic macrophytes – A review, *Ejfa* 24 (2012) 510–526. <https://doi.org/10.9755/ejfa.v24i6.510526>.
- [24] R.P. Sinha, D.-P. Häder, UV-induced DNA damage and repair: a review, *Photochem Photobiol Sci* 1 (2002) 225–236. <https://doi.org/10.1039/b201230h>.
- [25] E. Forján, I. Garbayo, M. Henriques, J. Rocha, J.M. Vega, C. Vílchez, UV-A Mediated Modulation of Photosynthetic Efficiency, Xanthophyll Cycle and Fatty Acid Production of *Nannochloropsis*, *Mar Biotechnol* 13 (2011) 366–375. <https://doi.org/10.1007/s10126-010-9306-y>.
- [26] L.S. Jahnke, Massive carotenoid accumulation in *Dunaliella bardawil* induced by ultraviolet-A radiation, *Journal of Photochemistry and Photobiology B: Biology* 48 (1999) 68–74. [https://doi.org/10.1016/S1011-1344\(99\)00012-3](https://doi.org/10.1016/S1011-1344(99)00012-3).
- [27] A. Salguero, R. León, A. Mariotti, B. De La Morena, J.M. Vega, C. Vílchez, UV-A mediated induction of carotenoid accumulation in *Dunaliella bardawil* with retention of cell viability, *Appl Microbiol Biotechnol* 66 (2005) 506–511. <https://doi.org/10.1007/s00253-004-1711-6>.
- [28] A.L. White, L.S. Jahnke, Contrasting Effects of UV-A and UV-B on Photosynthesis and Photoprotection of β -carotene in two *Dunaliella* spp., *Plant and Cell Physiology* 43 (2002) 877–884. <https://doi.org/10.1093/pcp/pcf105>.
- [29] D. Lean, Attenuation of Solar Radiation in Humic Waters, in: D.O. Hessen, L.J. Tranvik (Eds.), *Aquatic Humic Substances*, Springer Berlin Heidelberg, Berlin, Heidelberg, 1998: pp. 109–124. https://doi.org/10.1007/978-3-662-03736-2_6.

- [30] T. Nielsen, N.G.A. Ekelund, Influence of solar ultraviolet radiation on photosynthesis and motility of marine phytoplankton, *FEMS Microbiology Ecology* 18 (1995) 281–288. <https://doi.org/10.1111/j.1574-6941.1995.tb00184.x>.
- [31] G.H. Krause, E. Weis, Chlorophyll Fluorescence and Photosynthesis: The Basics, *Annu. Rev. Plant. Physiol. Plant. Mol. Biol.* 42 (1991) 313–349. <https://doi.org/10.1146/annurev.pp.42.060191.001525>.
- [32] U. Schreiber, W. Bilger, C. Neubauer, Chlorophyll Fluorescence as a Nonintrusive Indicator for Rapid Assessment of In Vivo Photosynthesis, in: E.-D. Schulze, M.M. Caldwell (Eds.), *Ecophysiology of Photosynthesis*, Springer Berlin Heidelberg, Berlin, Heidelberg, 1995: pp. 49–70. https://doi.org/10.1007/978-3-642-79354-7_3.
- [33] M. Consalvey, R.G. Perkins, D.M. Paterson, G.J.C. Underwood, PAM FLUORESCENCE: A BEGINNERS GUIDE FOR BENTHIC DIATOMISTS, *Diatom Research* 20 (2005) 1–22. <https://doi.org/10.1080/0269249X.2005.9705619>.
- [34] K. Maxwell, G.N. Johnson, Chlorophyll fluorescence—a practical guide, *Journal of Experimental Botany* 51 (2000) 659–668. <https://doi.org/10.1093/jexbot/51.345.659>.
- [35] N. Coulombier, E. Nicolau, L. Le Déan, C. Antheaume, T. Jauffrais, N. Lebouvier, Impact of Light Intensity on Antioxidant Activity of Tropical Microalgae, *Marine Drugs* 18 (2020) 122. <https://doi.org/10.3390/md18020122>.
- [36] R.E. Norris, T. Hori, M. Chihara, Revision of the genus *Tetraselmis* (Class Prasinophyceae), *Bot Mag Tokyo* 93 (1980) 317–339. <https://doi.org/10.1007/BF02488737>.
- [37] R. Cerezuela, F.A. Guardiola, P. González, J. Meseguer, M.Á. Esteban, Effects of dietary *Bacillus subtilis*, *Tetraselmis chuii*, and *Phaeodactylum tricornutum*, singularly or in combination, on the immune response and disease resistance of sea bream (*Sparus aurata* L.), *Fish & Shellfish Immunology* 33 (2012) 342–349. <https://doi.org/10.1016/j.fsi.2012.05.004>.
- [38] K. Goiris, K. Muylaert, I. Fraeye, I. Foubert, J. De Brabanter, L. De Cooman, Antioxidant potential of microalgae in relation to their phenolic and carotenoid content, *J Appl Phycol* 24 (2012) 1477–1486. <https://doi.org/10.1007/s10811-012-9804-6>.
- [39] E.C. Carballo-Cárdenas, P.M. Tuan, M. Janssen, R.H. Wijffels, Vitamin E (α -tocopherol) production by the marine microalgae *Dunaliella tertiolecta* and *Tetraselmis suecica* in batch cultivation, *Biomolecular Engineering* 20 (2003) 139–147. [https://doi.org/10.1016/S1389-0344\(03\)00040-6](https://doi.org/10.1016/S1389-0344(03)00040-6).
- [40] N. Coulombier, Evaluation des microalgues sélectionnées en Nouvelle-Calédonie comme source potentielle d'anti-oxydants naturels : identification des molécules anti-radicalaires et stimulation de leur biosynthèse par orientation métabolique, Université de la Nouvelle-Calédonie, 2020. <https://www.theses.fr/2020NCAL0002.pdf>.
- [41] P. Conan, F. Joux, J. Torréton, M. Pujo-Pay, T. Douki, E. Rochelle-Newall, X. Mari, Effect of solar ultraviolet radiation on bacterio- and phytoplankton activity in a large coral reef lagoon (southwest New Caledonia), *Aquat. Microb. Ecol.* 52 (2008) 83–98. <https://doi.org/10.3354/ame01204>.
- [42] P.R. Walne, *Experiments in the Large-scale Culture of the Larvae of Ostrea Edulis L.*, 3rd ed., H.M. Stationery Office, 1966.
- [43] R.J. Strasser, A. Srivastava, M. Tsimilli-Michael, The fluorescence transient as a tool to characterize and screen photosynthetic samples, in: 2000.
- [44] P.J. Ralph, R. Gademann, Rapid light curves: A powerful tool to assess photosynthetic activity, *Aquatic Botany* 82 (2005) 222–237. <https://doi.org/10.1016/j.aquabot.2005.02.006>.
- [45] G.H. Krause, E. Weis, Chlorophyll Fluorescence and Photosynthesis: The Basics, *Annu. Rev. Plant. Physiol. Plant. Mol. Biol.* 42 (1991) 313–349. <https://doi.org/10.1146/annurev.pp.42.060191.001525>.
- [46] U. Schreiber, New Emitter-Detector-Cuvette Assembly for Measuring Modulated Chlorophyll Fluorescence of Highly Diluted Suspensions in Conjunction with the Standard PAM Fluorometer, *Zeitschrift Für Naturforschung C* 49 (1994) 646–656. <https://doi.org/10.1515/znc-1994-9-1016>.

- [47] R.G. Perkins, J.-L. Mouget, S. Lefebvre, J. Lavaud, Light response curve methodology and possible implications in the application of chlorophyll fluorescence to benthic diatoms, *Mar Biol* 149 (2006) 703–712. <https://doi.org/10.1007/s00227-005-0222-z>.
- [48] P.J. Ralph, C. Wilhelm, J. Lavaud, T. Jakob, K. Petrou, S.A. Kranz, Fluorescence as a Tool to Understand Changes in Photosynthetic Electron Flow Regulation, in: D.J. Suggett, O. Prášil, M.A. Borowitzka (Eds.), *Chlorophyll a Fluorescence in Aquatic Sciences: Methods and Applications*, Springer Netherlands, Dordrecht, 2010: pp. 75–89. https://doi.org/10.1007/978-90-481-9268-7_4.
- [49] S. White, A. Anandraj, F. Bux, PAM fluorometry as a tool to assess microalgal nutrient stress and monitor cellular neutral lipids, *Bioresource Technology* 102 (2011) 1675–1682. <https://doi.org/10.1016/j.biortech.2010.09.097>.
- [50] J. Malapascua, C. Jerez, M. Sergejevová, F. Figueroa, J. Masojídek, Photosynthesis monitoring to optimize growth of microalgal mass cultures: application of chlorophyll fluorescence techniques, *Aquat. Biol.* 22 (2014) 123–140. <https://doi.org/10.3354/ab00597>.
- [51] S. Enríquez, M.A. Borowitzka, The Use of the Fluorescence Signal in Studies of Seagrasses and Macroalgae, in: D.J. Suggett, O. Prášil, M.A. Borowitzka (Eds.), *Chlorophyll a Fluorescence in Aquatic Sciences: Methods and Applications*, Springer Netherlands, Dordrecht, 2010: pp. 187–208. https://doi.org/10.1007/978-90-481-9268-7_9.
- [52] S. Beer, L. Axelsson, Limitations in the use of PAM fluorometry for measuring photosynthetic rates of macroalgae at high irradiances, *European Journal of Phycology* 39 (2004) 1–7. <https://doi.org/10.1080/0967026032000157138>.
- [53] P. Ralph, R. Gademann, A. Larkum, M. Kühl, Spatial heterogeneity in active chlorophyll fluorescence and PSII activity of coral tissues, *Marine Biology* 141 (2002) 639–646. <https://doi.org/10.1007/s00227-002-0866-x>.
- [54] R.J. Strasser, A. Srivastava, Govindjee, Polyphasic chlorophyll *a* fluorescence transient in plants and cyanobacteria*, *Photochemistry and Photobiology* 61 (1995) 32–42. <https://doi.org/10.1111/j.1751-1097.1995.tb09240.x>.
- [55] T. Platt, C.L. Gallegos, W.G. Harrison, Photoinhibition of photosynthesis in natural assemblages of marine phytoplankton, in: 1980.
- [56] J. Cosgrove, M.A. Borowitzka, Chlorophyll Fluorescence Terminology: An Introduction, in: D.J. Suggett, O. Prášil, M.A. Borowitzka (Eds.), *Chlorophyll a Fluorescence in Aquatic Sciences: Methods and Applications*, Springer Netherlands, Dordrecht, 2010: pp. 1–17. https://doi.org/10.1007/978-90-481-9268-7_1.
- [57] C.J. Williamson, R. Perkins, M.L. Yallop, C. Peteiro, N. Sanchez, K. Gunnarsson, M. Gamble, J. Brodie, Photoacclimation and photoregulation strategies of *Corallina* (Corallinales, Rhodophyta) across the NE Atlantic, *European Journal of Phycology* 53 (2018) 290–306. <https://doi.org/10.1080/09670262.2018.1442586>.
- [58] L. Van Heukelem, C.S. Thomas, Computer-assisted high-performance liquid chromatography method development with applications to the isolation and analysis of phytoplankton pigments, *Journal of Chromatography A* 910 (2001) 31–49. [https://doi.org/10.1016/S0378-4347\(00\)00603-4](https://doi.org/10.1016/S0378-4347(00)00603-4).
- [59] S. Madronich, R.L. McKenzie, L.O. Björn, M.M. Caldwell, Changes in biologically active ultraviolet radiation reaching the Earth's surface, *Journal of Photochemistry and Photobiology B: Biology* 46 (1998) 5–19. [https://doi.org/10.1016/S1011-1344\(98\)00182-1](https://doi.org/10.1016/S1011-1344(98)00182-1).
- [60] G. Döhler, G. Drebes, M. Lohmann, Effect of UV-A and UV-B radiation on pigments, free amino acids and adenylate content of *Dunaliella tertiolecta* Butcher (chlorophyta), *Journal of Photochemistry and Photobiology B: Biology* 40 (1997) 126–131. [https://doi.org/10.1016/S1011-1344\(97\)00037-7](https://doi.org/10.1016/S1011-1344(97)00037-7).
- [61] B. Mogedas, C. Casal, E. Forján, C. Vílchez, β -Carotene production enhancement by UV-A radiation in *Dunaliella bardawil* cultivated in laboratory reactors, *Journal of Bioscience and Bioengineering* 108 (2009) 47–51. <https://doi.org/10.1016/j.jbiosc.2009.02.022>.

- [62] M. Mutschlechner, A. Walter, L. Colleselli, C. Griesbeck, H. Schöbel, Enhancing carotenogenesis in terrestrial microalgae by UV-A light stress, *J Appl Phycol* 34 (2022) 1943–1955. <https://doi.org/10.1007/s10811-022-02772-5>.
- [63] J. Xu, K. Gao, UV-A enhanced growth and UV-B induced positive effects in the recovery of photochemical yield in *Gracilaria lemaneiformis* (Rhodophyta), *Journal of Photochemistry and Photobiology B: Biology* 100 (2010) 117–122. <https://doi.org/10.1016/j.jphotobiol.2010.05.010>.
- [64] A.C. Redfield, The Biological control of Chemical Factors in the environment, *American Scientist* 46 (1958) 230A–221.
- [65] S. Burkhardt, U. Riebesell, CO₂ availability affects elemental composition (C:N:P) of the marine diatom *Skeletonema costatum*, *Mar. Ecol. Prog. Ser.* 155 (1997) 67–76. <https://doi.org/10.3354/meps155067>.
- [66] H. Hillebrand, U. Sommer, The nutrient stoichiometry of benthic microalgal growth: Redfield proportions are optimal, *Limnol. Oceanogr.* 44 (1999) 440–446. <https://doi.org/10.4319/lo.1999.44.2.0440>.
- [67] U. Riebesell, Effects of CO₂ Enrichment on Marine Phytoplankton, *Journal of Oceanography* 60 (2004) 719–729. <https://doi.org/10.1007/s10872-004-5764-z>.
- [68] M.A. Brzezinski, THE Si:C:N RATIO OF MARINE DIATOMS: INTERSPECIFIC VARIABILITY AND THE EFFECT OF SOME ENVIRONMENTAL VARIABLES¹, *Journal of Phycology* 21 (2004) 347–357. <https://doi.org/10.1111/j.0022-3646.1985.00347.x>.
- [69] W. Darley, Biochemical composition, in: *The Biology of Diatoms.*, Blackwell Scientific Publications, Oxford, 1977: pp. 198–223.
- [70] G. Sarthou, K.R. Timmermans, S. Blain, P. Tréguer, Growth physiology and fate of diatoms in the ocean: a review, *Journal of Sea Research* 53 (2005) 25–42. <https://doi.org/10.1016/j.seares.2004.01.007>.
- [71] G. Britton, Structure and properties of carotenoids in relation to function., *The FASEB Journal* 9 (1995) 1551–1558. <https://doi.org/10.1096/fasebj.9.15.8529834>.
- [72] M. Takemura, T. Sahara, N. Misawa, Violaxanthin: natural function and occurrence, biosynthesis, and heterologous production, *Appl Microbiol Biotechnol* 105 (2021) 6133–6142. <https://doi.org/10.1007/s00253-021-11452-2>.
- [73] A.M. Gilmore, Mechanistic aspects of xanthophyll cycle-dependent photoprotection in higher plant chloroplasts and leaves, *Physiologia Plantarum* 99 (1997) 197–209. <https://doi.org/10.1111/j.1399-3054.1997.tb03449.x>.
- [74] F.J.L. Gordillo, C. Jiménez, J. Chavarría, F. Xavier Niell, Photosynthetic acclimation to photon irradiance and its relation to chlorophyll fluorescence and carbon assimilation in the halotolerant green alga *Dunaliella viridis*, *Photosynthesis Research* 68 (2001) 225–235. <https://doi.org/10.1023/A:1012969324756>.
- [75] T. Jauffrais, B. Jesus, V. Méléder, V. Turpin, A.D.P.G. Russo, P. Raimbault, V.M. Jézéquel, Physiological and photophysiological responses of the benthic diatom *Entomoneis paludosa* (Bacillariophyceae) to dissolved inorganic and organic nitrogen in culture, *Mar Biol* 163 (2016) 115. <https://doi.org/10.1007/s00227-016-2888-9>.
- [76] W.H. Jeffrey, D.L. Mitchell, Mechanisms of UV-Induced DNA Damage and Response in Marine Microorganisms, *Photochemistry and Photobiology* 65 (1997) 260–263. <https://doi.org/10.1111/j.1751-1097.1997.tb08555.x>.
- [77] E. Turcsányi, I. Vass, Inhibition of Photosynthetic Electron Transport by UV-A Radiation Targets the Photosystem II Complex¶, *Photochem Photobiol* 72 (2000) 513. [https://doi.org/10.1562/0031-8655\(2000\)072<0513:IOPETB>2.0.CO;2](https://doi.org/10.1562/0031-8655(2000)072<0513:IOPETB>2.0.CO;2).
- [78] I. Vass, E. Turcsányi, E. Touloupakis, D. Ghanotakis, V. Petrouleas, The Mechanism of UV-A Radiation-Induced Inhibition of Photosystem II Electron Transport Studied by EPR and Chlorophyll Fluorescence, *Biochemistry* 41 (2002) 10200–10208. <https://doi.org/10.1021/bi020272+>.

- [79] R.G. Perkins, J.-L. Mouget, S. Lefebvre, J. Lavaud, Light response curve methodology and possible implications in the application of chlorophyll fluorescence to benthic diatoms, *Mar Biol* 149 (2006) 703–712. <https://doi.org/10.1007/s00227-005-0222-z>.
- [80] J. Serôdio, S. Vieira, S. Cruz, Photosynthetic activity, photoprotection and photoinhibition in intertidal microphytobenthos as studied in situ using variable chlorophyll fluorescence, *Continental Shelf Research* 28 (2008) 1363–1375. <https://doi.org/10.1016/j.csr.2008.03.019>.
- [81] D.A. Christopher, J.E. Mullet, Separate Photosensory Pathways Co-Regulate Blue Light/Ultraviolet-A-Activated psbD-psbC Transcription and Light-Induced D2 and CP43 Degradation in Barley (*Hordeum vulgare*) Chloroplasts, *Plant Physiol.* 104 (1994) 1119–1129. <https://doi.org/10.1104/pp.104.4.1119>.
- [82] O. Zsiros, S.I. Allakhverdiev, S. Higashi, M. Watanabe, Y. Nishiyama, N. Murata, Very strong UV-A light temporally separates the photoinhibition of photosystem II into light-induced inactivation and repair, *Biochimica et Biophysica Acta (BBA) - Bioenergetics* 1757 (2006) 123–129. <https://doi.org/10.1016/j.bbabi.2006.01.004>.
- [83] R.J. Geider, J. Roche, R.M. Greene, M. Olaizola, RESPONSE OF THE PHOTOSYNTHETIC APPARATUS OF *PHAEODACTYLUM TRICORNUTUM* (BACILLARIOPHYCEAE) TO NITRATE, PHOSPHATE, OR IRON STARVATION1, *J Phycol* 29 (1993) 755–766. <https://doi.org/10.1111/j.0022-3646.1993.00755.x>.
- [84] J.A. Berges, D.O. Charlebois, D.C. Mauzerall, P.G. Falkowski, Differential Effects of Nitrogen Limitation on Photosynthetic Efficiency of Photosystems I and II in Microalgae, *Plant Physiol.* 110 (1996) 689–696. <https://doi.org/10.1104/pp.110.2.689>.
- [85] J.S. Cleveland, M.J. Perry, Quantum yield, relative specific absorption and fluorescence in nitrogen-limited *Chaetoceros gracilis*, *Mar. Biol.* 94 (1987) 489–497. <https://doi.org/10.1007/BF00431395>.
- [86] R.J. Strasser, M. Tsimilli-Michael, A. Srivastava, Analysis of the Chlorophyll a Fluorescence Transient, in: G.C. Papageorgiou, Govindjee (Eds.), *Chlorophyll a Fluorescence*, Springer Netherlands, Dordrecht, 2004: pp. 321–362. https://doi.org/10.1007/978-1-4020-3218-9_12.
- [87] C.-D. Jiang, G.-M. Jiang, X. Wang, L.-H. Li, D.K. Biswas, Y.-G. Li, Increased photosynthetic activities and thermostability of photosystem II with leaf development of elm seedlings (*Ulmus pumila*) probed by the fast fluorescence rise OJIP, *Environmental and Experimental Botany* 58 (2006) 261–268. <https://doi.org/10.1016/j.envexpbot.2005.09.007>.
- [88] J. Lavaud, P.G. Kroth, In Diatoms, the Transthylakoid Proton Gradient Regulates the Photoprotective Non-photochemical Fluorescence Quenching Beyond its Control on the Xanthophyll Cycle, *Plant and Cell Physiology* 47 (2006) 1010–1016. <https://doi.org/10.1093/pcp/pcj058>.
- [89] G. Perin, A. Bellan, A. Bernardi, F. Bezzo, T. Morosinotto, The potential of quantitative models to improve microalgae photosynthetic efficiency, *Physiol Plantarum* 166 (2019) 380–391. <https://doi.org/10.1111/ppl.12915>.
- [90] H. Wu, S. Roy, M. Alami, B.R. Green, D.A. Campbell, Photosystem II Photoinactivation, Repair, and Protection in Marine Centric Diatoms, *Plant Physiology* 160 (2012) 464–476. <https://doi.org/10.1104/pp.112.203067>.
- [91] N. Mariz-Ponte, R.J. Mendes, S. Sario, C.V. Correia, C.M. Correia, J. Moutinho-Pereira, P. Melo, M.C. Dias, C. Santos, Physiological, Biochemical and Molecular Assessment of UV-A and UV-B Supplementation in *Solanum lycopersicum*, *Plants* 10 (2021) 918. <https://doi.org/10.3390/plants10050918>.
- [92] L.A. Franklin, R.M. Forster, Review The changing irradiance environment: consequences for marine macrophyte physiology, productivity and ecology, *European Journal of Phycology* 32 (1997) 207–232.
- [93] P. Ahmad, C.A. Jaleel, M.A. Salem, G. Nabi, S. Sharma, Roles of enzymatic and nonenzymatic antioxidants in plants during abiotic stress, *Critical Reviews in Biotechnology* 30 (2010) 161–175. <https://doi.org/10.3109/07388550903524243>.

- [94] G. Malanga, S. Puntarulo, Oxidative stress and antioxidant content in *Chlorella vulgaris* after exposure to ultraviolet-B radiation, *Physiol Plant* 94 (1995) 672–679. <https://doi.org/10.1111/j.1399-3054.1995.tb00983.x>.
- [95] C. Faraloni, T. Di Lorenzo, A. Bonetti, Impact of Light Stress on the Synthesis of Both Antioxidants Polyphenols and Carotenoids, as Fast Photoprotective Response in *Chlamydomonas reinhardtii*: New Prospective for Biotechnological Potential of This Microalga, *Symmetry* 13 (2021) 2220. <https://doi.org/10.3390/sym13112220>.
- [96] C.H. Foyer, S. Shigeoka, Understanding Oxidative Stress and Antioxidant Functions to Enhance Photosynthesis, *Plant Physiology* 155 (2011) 93–100. <https://doi.org/10.1104/pp.110.166181>.
- [97] A. Smerilli, I. Orefice, F. Corato, A. Gavalás Olea, A.V. Ruban, C. Brunet, Photoprotective and antioxidant responses to light spectrum and intensity variations in the coastal diatom *Skeletonema marinoi*: Photoprotective network in *Skeletonema marinoi*, *Environ Microbiol* 19 (2017) 611–627. <https://doi.org/10.1111/1462-2920.13545>.
- [98] C.H. Foyer, Reactive oxygen species, oxidative signaling and the regulation of photosynthesis, *Environmental and Experimental Botany* 154 (2018) 134–142. <https://doi.org/10.1016/j.envexpbot.2018.05.003>.
- [99] M.A. Gururani, J. Venkatesh, L.S.P. Tran, Regulation of Photosynthesis during Abiotic Stress-Induced Photoinhibition, *Molecular Plant* 8 (2015) 1304–1320. <https://doi.org/10.1016/j.molp.2015.05.005>.
- [100] A. Smerilli, S. Balzano, M. Maselli, M. Blasio, I. Orefice, C. Galasso, C. Sansone, C. Brunet, Antioxidant and Photoprotection Networking in the Coastal Diatom *Skeletonema marinoi*, *Antioxidants* 8 (2019) 154. <https://doi.org/10.3390/antiox8060154>.

Appendix A. Supplementary material

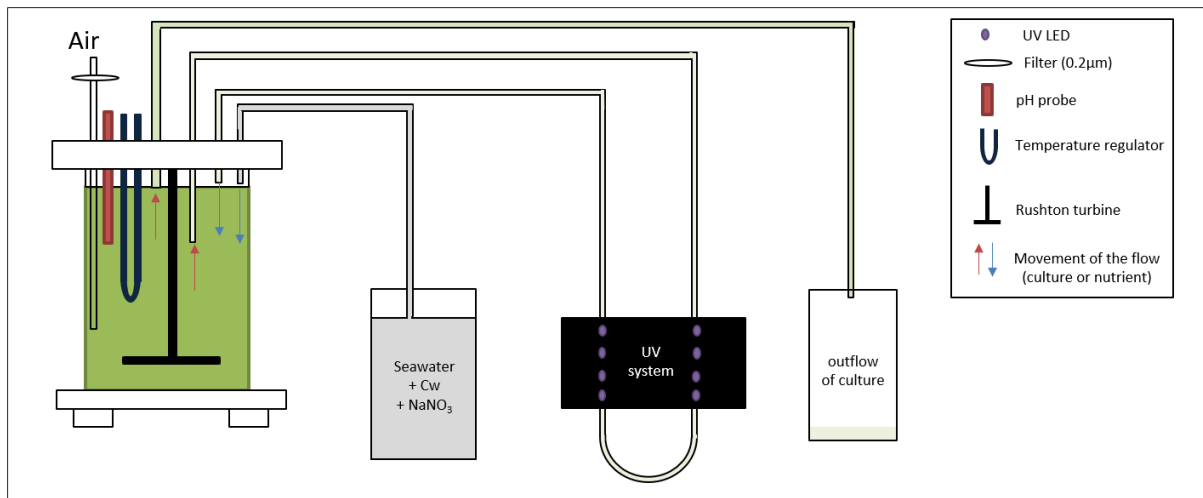


Fig. A 1. Scheme of the photobioreactor setup in a continuous mode (inflow of seawater, Conway -Cw- and NaNO₃ and outflow of culture) exposed to UV-A thanks to the UV system.

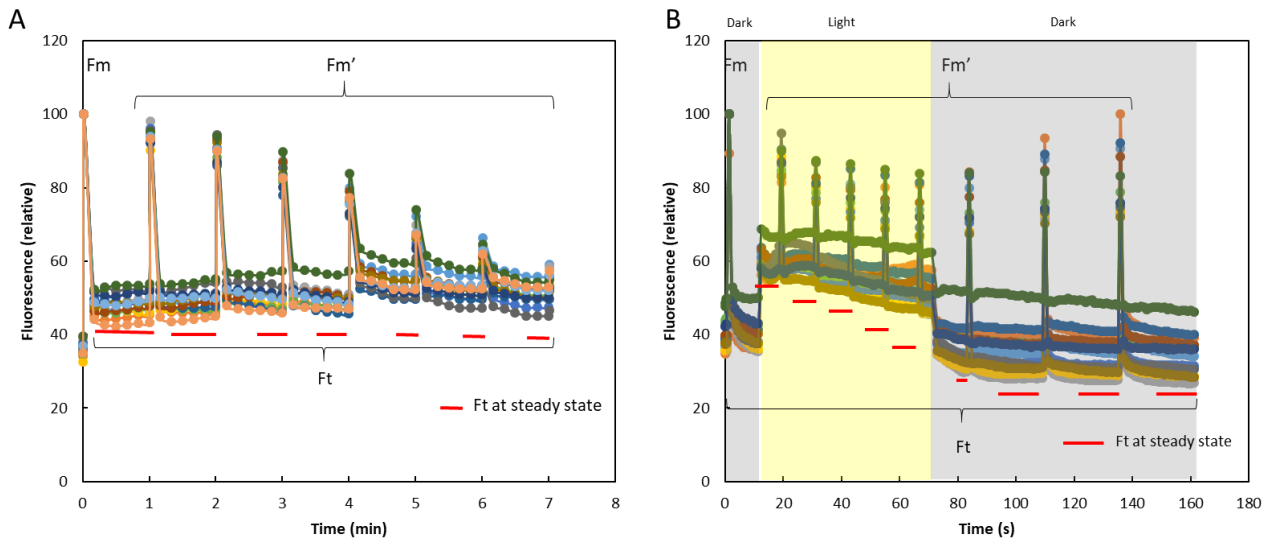


Fig. A2.: Relative fluorescence values during (A) RLCs and (B) NPQs assessment.

Table A1. Chemical composition of Conway Medium (Walne, 1966) [42]

Stocks		
Trace metal solution (1)		
ZnCl ₂	2.1	g
CoCl ₂ .6H ₂ O	2.0	g
(NH ₄) ₆ Mo ₇ O ₂₄ .4H ₂ O	0.9	g
CuSO ₄ .5H ₂ O	2.0	g
Distilled water	100.0	mL
Vitamin solution (2)		
Vitamin B ₁₂ (Cyanocobalamin)	10.0	mg
Vitamin B ₁ (Thiamine.HCl)	200.0	mg
Distilled water	100.0	mL
Nutrient solution (3)		
FeCl ₃ .6H ₂ O	1.3	g
MnCl ₂ .4H ₂ O	0.4	g
H ₃ BO ₃	33.5	g
EDTA (Disodium salt)	45.0	g
NaH ₂ PO ₄ .2H ₂ O	20.0	g
NANO ₃	100.0	g
Trace metal solution (1)	1.0	mL
Distilled water	1.0	L
Medium		
Nutrient solution (3)	1.0	mL
Vitamin solution (2)	0.1	mL
Sterilised seawater	1.0	L

Table A2. Results of Post hoc analysis (pairwise t-test) testing the differences times of exposure to UV-A on the maximum quantum yield (Fv/Fm) prior tested by one-way ANOVA analysis (*p-value* < 0.001). Differences were considered significant when *p-value* < 0.05 (bolded value).

	0	1	2	3	6	8
1	1.0					
2	1.0	1.0				
3	0.0011	< 0.001	< 0.001			
6	1.0	0.93	1.0	0.03		
8	1.0	1.0	1.0	< 0.001	0.66	
10	1.0	1.0	1.0	< 0.001	0.93	1.0

Table A3. Results of Post hoc analyses (pairwise t-test or Dunn test) testing the differences between times of exposure to UV-A on the OJIP parameters prior tested by one-way ANOVA or Kruskal Wallis analysis. Differences were considered significant when p- value < 0.050 (bolded value). * corresponds to non-parametric tests, Dunn test.

	1-0	3-0	10-0	3-1	10-1	10-3
Fv/Fm*	1.0	0.178	1.0	0.070	1.0	0.044
ϕ Eo	0.85	0.021	0.706	0.005	0.99	0.003
PI Abs	0.98	0.045	0.818	0.024	0.95	0.010
ABS/RC	1.0	0.015	0.925	0.014	0.93	0.005
DIo/RC*	1.0	0.253	0.895	0.087	1.0	0.022